

# GLOBAL OPTIMIZATION WITH ORTHOGONALITY CONSTRAINTS VIA STOCHASTIC DIFFUSION ON MANIFOLD

HONGLIN YUAN\*, XIAOYI GU\*, RONGJIE LAI<sup>†</sup>, AND ZAIWEN WEN<sup>‡</sup>

**Abstract.** Orthogonality constrained optimization is widely used in applications from science and engineering. Due to the nonconvex orthogonality constraints, many numerical algorithms often can hardly achieve the global optimality. We aim at establishing an efficient scheme for finding global minimizers under one or more orthogonality constraints. The main concept is based on noisy gradient flow constructed from stochastic differential equations (SDE) on the Stiefel manifold, the differential geometric characterization of orthogonality constraints. We derive an explicit representation of SDE on the Stiefel manifold endowed with a canonical metric and propose a numerically efficient scheme to simulate this SDE based on Cayley transformation with theoretical convergence guarantee. The convergence to global optimizers is proved under second-order continuity. The effectiveness and efficiency of the proposed algorithms are demonstrated on a variety of problems including homogeneous polynomial optimization, computation of stability number, and 3D structure determination from Common Lines in Cryo-EM.

**Key words.** Orthogonality constrained optimization, Global optimization, Stochastic differential equations, Stochastic diffusion on manifold

**AMS subject classifications.** 90C26, 65K05, 49Q99

**1. Introduction.** Mathematically, the orthogonality constrained problem can be formulated as the following form:

$$(1) \quad \min_{X \in \mathbb{R}^{n \times p}} \mathcal{F}(X), \quad \text{s.t. } X^\top X = I_p,$$

where  $\mathcal{F}$  is a smooth objective function and  $I_p$  indicates the  $p$ -by- $p$  identity matrix. The feasible set  $\mathcal{M}_{n,p} = \{X \in \mathbb{R}^{n \times p} : X^\top X = I_p\}$  is well-known as the Stiefel manifold (once equipped with its natural submanifold structure from  $\mathbb{R}^{n \times p}$ ). We also denote it by  $\mathcal{M}$  if there is no ambiguity on the dimensions.

Particularly in the case of  $p = 1$ , the above problem is known as the spherically constrained problem. In the case of  $p = n$ , the feasible set becomes orthogonal group  $\mathcal{O}_n$ , where the feasible matrices are square and orthogonal. More generally, the following optimization problem with multiple orthogonality (or spherical) constraints is widely used in many problems such as conformal mapping [12, 15], p-Harmonic flow [17, 32, 33, 11], 1-bit compressive sensing [4, 16], compressed modes [26], the graph stability number, Cryo-electron microscopy (Cryo-EM) [31], nonlinear eigenvalue problem in density functional theory [19, 35] as well as dictionary learning [2, 5]:

$$(2) \quad \min_{X_1 \in \mathbb{R}^{n_1 \times p_1}, \dots, X_q \in \mathbb{R}^{n_q \times p_q}} \mathcal{F}(X_1, \dots, X_q), \quad \text{s.t. } X_i^\top X_i = I_{p_i}, \quad i = 1, \dots, q.$$

Non-convexity is one of the major challenges of problems (1) and (2) since there might be multiple local minimizers, from which finding global minimizers is generally NP-hard. Most existing algorithms [1, 36, 23] on the Stiefel manifold focus on finding local optimizers without exploiting the global structures, and thus there is no guarantee to obtain the global minimizers except for some trivial cases.

\*Computational Mathematics, Peking University, China (yhlmath@pku.edu.cn, xiaoyigu@pku.edu.cn).

<sup>†</sup>Department of Mathematics, Rensselaer Polytechnic Institute, Troy, NY 12180 (lair@rpi.edu).

<sup>‡</sup>Beijing International Center for Mathematical Research, Peking University, China (wenzw@pku.edu.cn).

**1.1. Local feasible solver on Stiefel manifold.** One step of our algorithm is mostly based on the first-order algorithms proposed in [36], which we consider to have low computational cost and briefly describe here.

Given a point  $X$  on  $\mathcal{M}_{n,p}$ , the canonical metric  $g^c$  on the tangent space  $\mathcal{T}_X \mathcal{M}_{n,p} = \{Z \in \mathbb{R}^{n,p}, Z^\top X + X^\top Z = 0\}$  is defined as

$$g^c(Z_1, Z_2) := \text{tr}(Z_1^\top (I - \frac{1}{2}XX^\top)Z_2).$$

This metric considers the Stiefel manifold to be a quotient space  $M_{n,p} = O_n/O_{n-p}$ , in which  $O_k$  is the group of  $k \times k$  orthogonal matrices. Let us write  $G_{ij} = \partial_{ij}\mathcal{F}$ , then the gradient of  $\mathcal{F}$  with respect to  $g^c$  [1, 36] is given by

$$(3) \quad \nabla_{\mathcal{M}}^c \mathcal{F}(X) = G - XG^\top X.$$

Throughout the paper, we will always adopt the canonical metric, the superscript indicating the canonical metric will be omitted. Let  $A = GX^\top - XG^\top$ , the authors in [36] consider an implicit update scheme as

$$(4) \quad Y(\tau) = X - \tau A \left( \frac{X + Y(\tau)}{2} \right).$$

This leads to the following Cayley transformation,

$$(5) \quad Y(\tau) = (I + \frac{\tau}{2}A)^{-1} (I - \frac{\tau}{2}A)X.$$

It has been shown in [36] that the update scheme automatically preserve the orthogonality constraint due to the property of Cayley transformation. In addition, with certain conditions, it has also been proved in [36] that the sequence generated using this algorithm satisfying  $\lim_{k \rightarrow 0} \|\nabla F(X^k)\|_F = 0$ .

**1.2. Global optimization by diffusions.** For a general non-convex unconstrained optimization problem

$$(6) \quad \min_{x \in \mathbb{R}^n} f(x).$$

A well known method is to consider the gradient flow

$$(7) \quad dx(t) = -\nabla f(x(t))dt,$$

yet  $x(t)$  is often trapped at a local stationary point due to nonconvexity. A well-known remedy is to add white noise to the gradient flow [3, 6, 9, 10], allowing the trajectory to “climb over the mountains” and escape from the local minimizers. Mathematically, this type of methods can be formulated as the following *Stochastic Differential Equation* (SDE) [24]:

$$(8) \quad dx(t) = -\nabla f(x(t))dt + \sigma(t)dB(t),$$

where  $f(x)$  is the objective function defined on  $\mathbb{R}^n$  and  $B(t)$  is an  $n$ -dimensional standard Brownian motion, which is also known as the Wiener process. Different choices of  $\sigma(t)$  lead to different diffusion algorithms and different results. It has been proved in [6, 9] that if the diffusion strength  $\sigma(t)$  is chosen as  $\sigma(t) = c/\sqrt{\log(t+2)}$  for some  $c \geq c_0$ , referred as *Continuous Diminishing Diffusion* (CDD, also known as

*Simulated Annealing*),  $x(t)$  converges to the set of global minimizers under appropriate conditions on  $f$ . In [9], the objective function is defined on a compact set, while the assumption is lifted in [6]. Other choices of the diffusion strength  $\sigma(t)$  are discussed in several articles. The properties with large  $\sigma(t)$  is discussed in [37]. More recently, a method called intermittent diffusion (ID) has been proposed in [7], where a piecewise constant diffusion strength  $\sigma(t) = \sum_{i=1}^N \sigma_i I_{[S_i, S_i+T_i]}(t)$  is considered. In other words, this method essentially considers to alternatively update variables between gradient descent and noisy gradient descent. It has been shown in [7] the global convergence ID and its effectiveness in specific problems.

To the best of our knowledge, only a few articles apply the SDE method to constrained problems. Problems with linear constrained is discussed in [29]. Portfolio selection having higher order moments with selected constraints is studied in [20]. The authors in [30] apply the method to robust chance constraint problems and a class of minimax problems is solved in [27]. In [28], problems with equality constraints are solved but no theoretical validation is provided that the constraints can be preserved using the proposed SDE.

**1.3. Main Results.** In order to find the global minimizers of orthogonality constrained problems, it is natural to consider a generalization of the diffusion methods based on (8) in Euclidean space to problems with orthogonality constraints (1). Our strategy is a combination of the CDD and ID, which leads to an optimization procedure that alternatively apply the diminishing diffusion and the deterministic local solver mentioned in subsection 1.1. We refer this procedure as an intermittent diminishing diffusion on manifold (IDDM). One crucial step of IDDM is to explore an computational tractable method to the SDE on the Stiefel manifold, which can be symbolically written as follows:

$$(9) \quad dX(t) = -\nabla_{\mathcal{M}}\mathcal{F}(X(t))dt + \sigma(t) \circ dB_{\mathcal{M}}(t),$$

where  $\nabla_{\mathcal{M}}$  and  $B_{\mathcal{M}}$  stand for gradient and Wiener process on manifold, respectively. One of the major challenges of using the above equation on the Stiefel manifold is the lack of global parameterization of the manifold, which make the numerical computation not straightforward to generate Wiener process on the Stiefel manifold. On the other hand,  $\mathcal{M}_{n,p}$  is an embedding manifold in  $\mathbb{R}^{n,p}$ , whose embedding coordinates can be used to design an extrinsic form of the above SDE. In order to make use of (9) on numerical optimization, we propose an extrinsic presentation to facilitate numerical work. Our idea is to project the Brownian motion in the ambient space to the tangent space of  $\mathcal{M}_{n,p}$ . Based on this idea, we have theoretically validate the proposed procedure of IDDM for orthogonality constrained problems. More specifically, we have established the following results:

1. We theoretically show that the proposed extrinsic form is in fact generating feasible path constrained on  $\mathcal{M}_{n,p}$ .
2. We also validate that the proposed method of projection Brownian motion in  $\mathbb{R}^{n,p}$  to the tangent space of  $\mathcal{M}_{n,p}$  is an extrinsic form of the Brownian motion on the  $\mathcal{M}_{n,p}$ .
3. We further propose a numerical-efficient scheme to solve the proposed extrinsic equation and theoretically validate the half-order convergence of the scheme.
4. We also provide theoretical global convergence analysis of the proposed method, which is a consequence that the proposed extrinsic form satisfies the associated Fokker-Planck equation on the manifold. ■

5. We numerically demonstrate that often only a few cycles of IDDM is needed to identify a better solution than the local algorithm for difficult problems with multiple local minimizers.

The rest of this paper is organized as follows. In section 2, we propose an extrinsic form of the SDE (9) and discuss its well-posedness. We also show the proposed extrinsic diffusion term in fact provides the Brownian motion on the Steifel manifold. Numerical scheme of solving the proposed SDE and its convergence is discussed in section 3. After that, we describe the proposed intermittent diminishing diffusion on manifold (IDDM) and show that IDDM converges to global optimizers of the orthogonality constrained problems with probability almost equal to 1 in section 4. Numerically we demonstrate the effectiveness of the proposed method on several applications involving orthogonality constrained optimization in section 5. Finally, we conclude our work in section 6.

**2. SDE on Stiefel manifold.** In this section, we propose an explicit representation of the SDE (9). We also validate that the proposed explicit form is well-posed by showing that solutions of the explicit form stay on the Stiefel manifold with probability 1. We further show that the proposed method of projecting Brownian motion is a Brownian motion on the Stiefel manifold.

As we mentioned in the introduction, one crucial step of adapting SDE methods to the orthogonality constrained problems is how to design a computation tractable way of generating Brownian motion on the Stiefel manifold. Note that for any matrix  $Z \in \mathbb{R}^{n \times p}$ , we can use the following operator to project  $Z$  to  $\mathcal{T}_X \mathcal{M}_{n,p}$ .

$$(10) \quad P : \mathbb{R}^{n \times p} \rightarrow \mathcal{T}_X \mathcal{M}_{n,p}, \quad Y \mapsto P_X(Z) = Z - \alpha X Z^\top X - \beta X X^\top Z$$

where  $\alpha = \sqrt{2}/2$ ,  $\beta = 1 - \sqrt{2}/2$ . This motivates us to project the Brownian motion in the ambient space to the tangent space of  $\mathcal{M}_{n,p}$  based on this projection operator. Namely, we propose the extrinsic representation of the SDE (9) on Stiefel manifold as

$$(11) \quad dX(t) = -\nabla_{\mathcal{M}} \mathcal{F}(X(t)) dt + \sigma(t) \sum_{u=1}^n \sum_{v=1}^p P_{uv}(X(t)) \circ dB_{uv}(t),$$

where  $\{B_{uv}(t)\}$  is a series of (independent) one-dimensional standard Brownian motion, and  $P_{uv}$  is defined by

$$(12) \quad P_{uv}(X) = E_{uv} - \alpha X E_{uv}^\top X - \beta X X^\top E_{uv}, \quad X \in \mathcal{M}_{n,p}, \\ u = 1, 2, \dots, n, \quad v = 1, 2, \dots, p.$$

**2.1. Well-posedness of the extrinsic SDE.** There are several issues with respect to (11) to be clarified. First, the definition of coefficients of drift term and diffusion term is restricted to the manifold, and thus a proper extension is needed in order to make it a well-posed SDE in Euclidean space  $\mathbb{R}^{n \times p}$ . We first show that the SDE given by (11) is well-posed. In other words, there is an equivalent extension to the euclidean space  $\mathbb{R}^{n \times p}$  that exists, lies on the manifold and gives a unique solution. We also expect that the solution will not leave the manifold so that the off-manifold coefficient will not impact the solution. The answers of all the above concerns are addressed in the following theorem.

**THEOREM 1.** *Let  $V$  be an arbitrary smooth vector field on the Stiefel manifold  $\mathcal{M}_{n,p}$ . Then*

- (a) *There exists some smooth extensions of  $V(X)$  and  $P_{uv}(X)$  in  $\mathbb{R}^{n \times p}$  (denoted by  $\tilde{V}(X)$  and  $\tilde{P}_{uv}(X)$ ), which are globally Lipschitz. Hence, there exists a unique solution  $X(t, w)$  for the extended SDE*

$$(13) \quad dX(t) = \tilde{V}(X(t))dt + \sigma(t) \sum_{u=1}^n \sum_{v=1}^p \tilde{P}_{uv}(X(t)) \circ dB_{uv}(t).$$

in  $\mathbb{R}^{n \times p}$  once the extension is fixed.

- (b) *Let  $X(t)$  be the solution of (13), and then  $X(t)$  almost surely stays on  $\mathcal{M}_{n,p}$  provided it originate on the manifold, i.e.,*

$$(14) \quad \mathbb{P}\{X(t) \in \mathcal{M}_{n,p} | X(0) \in \mathcal{M}_{n,p}\} = 1, \quad \forall t \geq 0.$$

*In addition,  $X(t)$  does not leave its connected component in the case of  $n = p$ , i.e.,*

$$\mathbb{P}\{\det(X(t)) = \det(X(0)) | X(0) \in \mathcal{M}_{n,n}\} = 1, \quad \forall t \geq 0.$$

*The solution of (13) is unique regardless of the extension of  $V$  and  $P_{uv}$ .*

*Proof.* (a) Direct observation suggests that  $\mathcal{M}_{n,p}$  is a compact subset of  $\mathbb{R}^{n \times p}$ , which makes it possible to construct a globally Lipschitz extension. The extension is not unique, and for example we can take

$$(15) \quad \begin{cases} \tilde{V}(X) := \zeta_\varepsilon(\|X^\top X - I_p\|_2^2) V(Q(X)), \\ \tilde{P}_{uv}(X) := \zeta_\varepsilon(\|X^\top X - I_p\|_2^2) (E_{uv} - \alpha X E_{uv}^\top X - \beta X X^\top E_{uv}), \end{cases}$$

where  $Q(X)$  indicates the  $n$ -by- $p$  matrix from reduced  $QR$  decomposition of  $X$  (here we follow the convention that the diagonal entries of upper triangular  $R$  are non-negative).  $\zeta_\varepsilon$  is a  $C_0^\infty([0, +\infty))$  mollifier satisfying

$$(16) \quad \zeta_\varepsilon([0, \varepsilon]) \equiv 1, \quad \zeta_\varepsilon([2\varepsilon, +\infty)) \equiv 0,$$

where  $\varepsilon$  is a given positive constant with  $\varepsilon < 1/2$ . Under this condition one can show that both  $\tilde{V}$  and  $\tilde{P}_{ij}$  are globally Lipschitz. The existence and uniqueness of (13) follow directly from the existence and uniqueness theorem of general SDE (see Theorem 5.2.1 of [24] for example).

- (b) The general feasibility results (14) can be derived by viewing (13) as a process driven by  $\mathbb{R}^{np+1}$ -valued semimartingale  $Z(t) = (t, \sigma(t)B_{ij}(t))$  and applying Proposition 1.2.8 of [14]. The special case of  $n = p$  can be treated similarly but viewing two connected components as two separate manifolds instead. The uniqueness can be referred to Theorem 1.2.9 of [14].  $\square$

In view of the uniqueness result we can specify that the extension of  $\tilde{V}$  and  $\tilde{P}_{uv}$  is given by (15) to facilitate further discussion. Sometimes it would be more convenient to analyze the Ito version of (13), which can be derived from the following transformation property between Ito SDE and Stratonovich SDE in the Euclidean space.

LEMMA 2 ([24]). *The corresponding Ito version of Stratonovich system*

$$dX_\eta(t) = h_\eta(X(t), t)dt + \sum_{\lambda} H_{\eta\lambda}(X(t), t) \circ dB_\lambda(t)$$

is given by

$$(17) \quad dX_\eta(t) = \left[ h_\eta(X(t), t) + \frac{1}{2} \sum_\lambda \left( \sum_\mu \frac{\partial H_{\eta\lambda}}{\partial X_\mu} H_{\mu\lambda} \right) \right] dt + \sum_\lambda H_{\eta\lambda}(X(t), t) dB_\lambda(t).$$

Based on this lemma, we can derive the Ito version of the Stratonovich SDE (13) described in the following theorem.

**THEOREM 3.** *The corresponding Ito version of Stratonovich SDE (13) on  $\mathcal{M}_{n,p}$  (with feasible initial point  $X(0) \in \mathcal{M}_{n,p}$ ) is given by*

$$(18) \quad \begin{aligned} dX(t) = & \left( V(X(t)) - \frac{n-1}{2} \sigma^2(t) X(t) \right) dt \\ & + \sigma(t) \sum_{u=1}^n \sum_{v=1}^p (E_{uv} - \alpha X E_{uv}^\top X - \beta X X^\top E_{uv}) dB_{uv}(t). \end{aligned}$$

Here we omit the discussion of definition of parameters outside the manifold.

*Proof.* Write (13) coordinate-wise as

$$\begin{aligned} dX_{ij}(t) = & \tilde{V}_{ij}(X) dt + \sigma(t) \sum_{u=1}^n \sum_{v=1}^p [\zeta_\varepsilon(\|X^\top X - I_p\|_2^2) \\ & (\delta_{iu} \delta_{jv} - \alpha X_{iv} X_{uj} - \beta \sum_{w=1}^p X_{iw} X_{uw} \delta_{jv}) \circ dB_{uv}(t)]. \end{aligned}$$

Applying Lemma 2 by viewing the index  $\eta = (i, j)$  and  $\lambda = (u, v)$ , one can show that the  $(i, j)$ -th entry of the additional drift term is given by

$$(19) \quad \begin{aligned} & \frac{1}{2} \sigma^2(t) \sum_{u,v,s,t} \left[ \partial_{st} (-\alpha X_{iv} X_{uj} - \beta \sum_{w=1}^p X_{iw} X_{uw} \delta_{jv}) \right. \\ & \quad \left. \cdot (\delta_{us} \delta_{vt} - \alpha X_{sv} X_{ut} - \beta \sum_{w=1}^p X_{sw} X_{uw} \delta_{vt}) \right] \\ & = \frac{1}{2} \sigma^2(t) \sum_{u,v,s,t} [(-\alpha \delta_{is} \delta_{vt} X_{uj} - \alpha \delta_{us} \delta_{jt} X_{iv} - \beta \delta_{is} \delta_{jv} X_{ut} - \beta \delta_{jv} \delta_{us} X_{it}) \\ & \quad \cdot (\delta_{us} \delta_{vt} - \alpha X_{sv} X_{ut} - \beta \sum_{w=1}^p X_{sw} X_{uw} \delta_{vt})] \\ & = \frac{1}{2} \sigma^2(t) [(2\alpha^2 + \beta^2 + \alpha\beta - \beta) - (\alpha + \beta)n + (\beta^2 + 3\alpha\beta - \alpha)p] X_{ij} \\ & = -\frac{(n-1)}{2} \sigma^2(t) X_{ij}. \end{aligned} \quad \square$$

Here we omit the discussion of coefficients off the manifold as the derivation of the mollifier  $\eta_\varepsilon$  will not affect the on-manifold result due to the hypothesis of (16). In addition, the second last equality of the above derivation is provided by simply expanding each item of (19) using the facts  $\sum_u X_{ui} X_{uj} = \delta_{ij}$  and  $\sum_{uv} X_{uv}^2 = p$ . More specifically, we summarize products among pairs in the following table:

$\times$	$\delta_{us}\delta_{vt}$	$-\alpha X_{sv}X_{ut}$	$-\beta \sum_{w=1}^p X_{sw}X_{uw}\delta_{vt}$
$-\alpha \sum_{u,v,s,t} \delta_{is}\delta_{vt}X_{uj}$	$-\alpha pX_{ij}$	$\alpha^2 X_{ij}$	$\alpha\beta pX_{ij}$
$-\alpha \sum_{u,v,s,t} \delta_{us}\delta_{jt}X_{iv}$	$-\alpha nX_{ij}$	$\alpha^2 X_{ij}$	$\alpha\beta pX_{ij}$
$-\beta \sum_{u,v,s,t} \delta_{is}\delta_{jv}X_{ut}$	$-\beta X_{ij}$	$\alpha\beta pX_{ij}$	$\beta^2 X_{ij}$
$-\beta \sum_{u,v,s,t} \delta_{jv}\delta_{us}X_{it}$	$-\beta nX_{ij}$	$\alpha\beta X_{ij}$	$\beta^2 pX_{ij}$

REMARK 4. Using the projection operator defined in (10), we can simplify the notation by writing the diffusion term in short as

$$(20) \quad \sum_{u=1}^n \sum_{v=1}^p (E_{uv} - \alpha X E_{uv}^\top X - \beta X X^\top E_{uv}) dB_{uv}(t) = P_X(dB(t)).$$

For example, the above Ito SDE (18) can be simplified as

$$(21) \quad dX(t) = \left( V(X(t)) - \frac{n-1}{2} \sigma^2(t) X(t) \right) dt + \sigma(t) P_X(dB(t)).$$

We will follow this convention throughout the paper.

**2.2. Laplace-Beltrami Operator on Canonical Stiefel Manifold.** It remains to show that the diffusion term of extrinsic SDE (13) is the Brownian motion on the Stiefel manifold. Before considering that, we first provide an extrinsic representation of the Laplace-Beltrami (LB) operator on the Stiefel manifold.

THEOREM 5 (Extrinsic form of the LB operator on  $\mathcal{M}_{n,p}$ ). *The LB operator at  $X$  on  $\mathcal{M}_{n,p}$  (endowed with the canonical metric) is given by*

$$(22) \quad \Delta_{\mathcal{M}_{n,p}} = \sum_{i=1}^n \sum_{j=1}^p \partial_{ij}^2 - \sum_{i,u=1}^n \sum_{j,v=1}^p X_{iv}X_{uj} \partial_{ij} \partial_{uv} - (n-1) \sum_{i=1}^n \sum_{j=1}^p X_{ij} \partial_{ij}.$$

We calculate the LB operator using the trace of the Hessian operator along an orthonormal basis in the tangent space  $\mathcal{T}_X \mathcal{M}_{n,p}$ . First, we provide an orthonormal basis in the following lemma.

LEMMA 6 (Orthonormal basis of  $\mathcal{T}_X \mathcal{M}_{n,p}$ ). *Let  $Q$  to be an extended orthogonal matrix of  $X$ , such that  $Q \in \mathbb{R}^{n \times n}$ ,  $Q^\top Q = I_n$  and  $Q = [X, X_\perp]$ . An orthonormal basis of  $\mathcal{T}_X \mathcal{M}_{n,p}$  is given by*

$$\begin{aligned} U_{ij} &= Q(E_{ij} - E_{ji}), & i < j \leq p, \\ U_{ij} &= QE_{ij}, & i > p, \end{aligned}$$

where  $E_{ij}$  is the element matrix in  $\mathbb{R}^{n \times p}$ . The set of the basis is denoted by  $\Lambda$ .

*Proof of Lemma 6.* To simplify the notation, we set  $\tilde{E}_{ij} = E_{ij} - E_{ji}$ , ( $i, j \leq p$ ) or  $\tilde{E}_{ij} = E_{ij}$ , ( $i > p$ ). The orthogonality of  $Q$  indicates that  $\Lambda$  is linear independent. It can be easily calculated that  $\Lambda$  has  $np - p(p+1)/2$  elements so that  $\Lambda$  spans  $\mathcal{T}_X \mathcal{M}_{n,p}$ . We next calculate the inner product as

$$\begin{aligned} g^c(U_{ij}, U_{kl}) &= \text{tr} \left( \tilde{E}_{ij}^\top \text{diag} \left\{ \frac{1}{2} I_p, I_n \right\} \tilde{E}_{kl} \right) = 0, & \text{if } (i, j) \neq (k, l) \text{ and } (j, i) \neq (l, k); \\ g^c(U_{ij}, U_{ij}) &= \text{tr} \left( \tilde{E}_{ij}^\top \text{diag} \left\{ \frac{1}{2} I_p, I_n \right\} \tilde{E}_{ij} \right) = 1, & \text{if } i \neq j; \end{aligned}$$

The results above indicate that  $\Lambda$  is the set of orthonormal basis of  $\mathcal{T}_X \mathcal{M}_{n,p}$ .  $\square$

From the orthonormal basis we can calculate the LB operator  $\Delta_{\mathcal{M}_{n,p}}$ .

*Proof of Theorem 5.* It has been shown in [8] that

$$(23) \quad \begin{aligned} \nabla_{\mathcal{M}_{n,p}}^2 \mathcal{F}(Z_1, Z_2) &= \nabla_E^2 \mathcal{F}(Z_1, Z_2) + \frac{1}{2} \text{tr}(G^\top Z_1 X^\top Z_2 + X^\top Z_1 G^\top Z_2) \\ &\quad - \frac{1}{2} \text{tr}((X^\top G + G^\top X) Z_1^\top (I - X X^\top) Z_2), \quad Z_1, Z_2 \in \mathcal{T}_X \mathcal{M}_{n,p}, \end{aligned}$$

where  $\nabla_E^2$  is the Hessian operator in the Euclidean space  $\mathbb{R}^{n \times p}$  and  $G_{ij} = \partial_{ij} \mathcal{F}$ .

From the orthonormal basis we obtain

$$\begin{aligned} \nabla_{\mathcal{M}_{n,p}}^2 \mathcal{F}(U_{ij}, U_{ij}) &= \nabla_E^2 \mathcal{F}(Q \tilde{E}_{ij}, Q \tilde{E}_{ij}) + \text{tr}(G^\top Q \tilde{E}_{ij} X^\top Q \tilde{E}_{ij}) \\ &\quad - \frac{1}{2} \text{tr}((X^\top G + G^\top X) \tilde{E}_{ij}^\top Q^\top (I - X X^\top) Q \tilde{E}_{ij}) \\ &= \nabla_E^2 \mathcal{F}(Q \tilde{E}_{ij}, Q \tilde{E}_{ij}) + \text{tr}(G^\top Q \tilde{E}_{ij} [I_p, 0_{p \times (n-p)}] \tilde{E}_{ij}) \\ &\quad - \frac{1}{2} \text{tr}((X^\top G + G^\top X) \tilde{E}_{ij}^\top \text{diag}\{0_p, I_{n-p}\} \tilde{E}_{ij}). \end{aligned}$$

Hence, we have

$$\begin{aligned} \Delta_{\mathcal{M}_{n,p}} \mathcal{F} &= \sum_{U_{ij} \in \Lambda} \nabla_{\mathcal{M}_{n,p}}^2 \mathcal{F}(U_{ij}, U_{ij}) \\ &= \sum_{i>p} [\nabla_E^2 \mathcal{F}(Q E_{ij}, Q E_{ij}) + 0 - \frac{1}{2} \text{tr}((X^\top G + G^\top X) E_{jj}^p)] \\ &\quad + \sum_{i<j \leq p} [\nabla_E^2 \mathcal{F}(Q \tilde{E}_{ij}, Q \tilde{E}_{ij}) + \text{tr}(G^\top Q \tilde{E}_{ij} [I_p, 0_{p \times (n-p)}] \tilde{E}_{ij}) - 0] \\ &= \sum_{i>p} [\nabla_E^2 \mathcal{F}(Q E_{ij}, Q E_{ij}) - (G^\top X)_{jj}] \\ &\quad + \sum_{i<j \leq p} [(\nabla_E^2 \mathcal{F}(Q E_{ij}, Q E_{ij}) + \nabla_E^2 \mathcal{F}(Q E_{ji}, Q E_{ji}) - 2 \nabla_E^2 \mathcal{F}(Q E_{ij}, Q E_{ji})) \\ &\quad - ((G^\top X)_{ii} + (G^\top X)_{jj})] \\ &= \sum_{i,j} \nabla_E^2 \mathcal{F}(Q E_{ij}, Q E_{ij}) - \sum_{i,j \leq p} \nabla_E^2 \mathcal{F}(Q E_{ij}, Q E_{ji}) - (n-1) \text{tr}(G^\top X). \end{aligned}$$

Orthogonal  $Q$  indicates that the linear transformation  $V \in \mathbb{R}^{n \times p} \mapsto QV \in \mathbb{R}^{n \times p}$  is orthogonal (under Euclidean metric). Therefore,

$$\begin{aligned} \Delta_{\mathcal{M}_{n,p}} \mathcal{F} &= \sum_{i,j} \nabla_E^2 \mathcal{F}(Q E_{ij}, Q E_{ij}) - \sum_{i,j \leq p} \nabla_E^2 \mathcal{F}(Q E_{ij}, Q E_{ji}) - (n-1) \text{tr}(G^\top X) \\ &= \Delta_E \mathcal{F} - \sum_{i,j \leq p} \nabla_E^2 \mathcal{F}(X E_{ij}^p, X E_{ji}^p) - (n-1) \text{tr}(G^\top X), \end{aligned}$$

where  $E_{ij}^p$  is the element matrix in  $\mathbb{R}^{p \times p}$ . With some expansion and mark changing, we obtain

$$\Delta_{\mathcal{M}_{n,p}} = \sum_{i=1}^n \sum_{j=1}^p \partial_{ij}^2 - \sum_{i,u=1}^n \sum_{j,v=1}^p X_{iv} X_{uj} \partial_{ij} \partial_{uv} - (n-1) \sum_{i=1}^n \sum_{j=1}^p X_{ij} \partial_{ij},$$

which completes the proof.  $\square$



### 2.3. Extrinsic formulation of Brownian motion on the Stiefel Manifold.

We now show that the diffusion term introduced in (13) is exactly the  $\mathcal{M}$ -valued Brownian motion driven by half of the Laplace-Beltrami operator. We state the result in the following theorem.

**THEOREM 7.** *Suppose that  $W(t)$  is the solution of the following SDE*

$$(24) \quad dW(t) = \sum_{u=1}^n \sum_{v=1}^p (E_{uv} - \alpha W E_{uv}^\top W - \beta W W^\top E_{uv}) \circ dB_{uv}(t).$$

Then  $W(t)$  is driven by half of Laplacian-Beltrami operator  $\Delta_{\mathcal{M}_{n,p}}$  on Stiefel Manifold, i.e.,

$$\frac{1}{2} \Delta_{\mathcal{M}_{n,p}} \varphi(W(t)) = \mathcal{L} \varphi(W(t)) := \lim_{t \rightarrow 0^+} \frac{\mathbb{E}[\varphi(W(t)) | W(0) = w_0] - \varphi(w_0)}{t}.$$

*Proof.* From Theorem 3, the Ito version of (24) is

$$dW(t) = -\frac{n-1}{2} X dt + \sum_{u=1}^n \sum_{v=1}^p (E_{uv} - \alpha W E_{uv}^\top W - \beta W W^\top E_{uv}) dB_{uv}(t).$$

The generator of  $\varphi$  can be derived as [24]

$$\begin{aligned} \mathcal{L} \varphi = & -\frac{n-1}{2} \sum_{i=1}^n \sum_{j=1}^p X_{ij} \partial_{ij} \varphi + \frac{1}{2} \sum_{i,u,s}^n \sum_{j,v,t}^p \left( \delta_{is} \delta_{jt} - \alpha X_{it} X_{sj} - \beta \sum_w^p X_{iw} X_{sw} \delta_{tj} \right) \\ & \cdot \left( \delta_{us} \delta_{vt} - \alpha X_{ut} X_{sv} - \beta \sum_z^p X_{uz} X_{sz} \delta_{tv} \right) \partial_{ij} \partial_{uv} \varphi. \end{aligned}$$

We expand pairwise products in the second term of the above equation as follows:

$$\begin{aligned} & \sum_{i,j,u,v,s,t} (\delta_{is} \delta_{jt}) (\delta_{us} \delta_{vt}) (\partial_{ij} \partial_{uv} \varphi) = \sum_{i,j} \partial_{ij}^2 \varphi, \\ & \sum_{i,j,u,v,s,t} (\delta_{is} \delta_{jt}) (-\alpha X_{ut} X_{sv}) (\partial_{ij} \partial_{uv} \varphi) = -\alpha \sum_{i,j,u,v} X_{uj} X_{iv} (\partial_{ij} \partial_{uv} \varphi), \text{ (twice)} \\ & \sum_{i,j,u,v,s,t} (\delta_{is} \delta_{jt}) (-\beta \sum_{z=1}^p X_{uz} X_{sz} \delta_{tv}) (\partial_{ij} \partial_{uv} \varphi) = -\beta \sum_{i,j,u,v} X_{iv} X_{uv} (\partial_{ij} \partial_{uv} \varphi), \text{ (twice)} \\ & \sum_{i,j,u,v,s,t} (-\alpha X_{it} X_{sj}) (-\alpha X_{ut} X_{sv}) (\partial_{ij} \partial_{uv} \varphi) = \alpha^2 \sum_{i,j,u,v} X_{iv} X_{uv} (\partial_{ij} \partial_{uv} \varphi), \\ & \sum_{i,j,u,v,s,t} (-\alpha X_{it} X_{sj}) (-\beta \sum_{z=1}^p X_{uz} X_{sz} \delta_{tv}) (\partial_{ij} \partial_{uv} \varphi) = \alpha \beta \sum_{i,j,u,v} X_{iv} X_{uj} (\partial_{ij} \partial_{uv} \varphi), \text{ (twice)} \\ & \sum_{i,j,u,v,s,t} (-\beta \sum_{w=1}^p X_{iw} X_{sw} \delta_{tj}) (-\beta \sum_{z=1}^p X_{uz} X_{sz} \delta_{tv}) (\partial_{ij} \partial_{uv} \varphi) \\ & = \beta^2 \sum_{i,j,u} (X X^\top X X^\top)_{iu} (\partial_{ij} \partial_{uj} \varphi) = \beta^2 \sum_{i,j,u,v} X_{iv} X_{uv} (\partial_{ij} \partial_{uj} \varphi). \end{aligned}$$

Hence, we have

$$\begin{aligned} \mathcal{L}\varphi = & -\frac{n-1}{2} \sum_{i=1}^n \sum_{j=1}^p X_{ij} \partial_{ij} \varphi + \frac{1}{2} \left[ \sum_{i,j} \partial_{ij}^2 \varphi + (-2\alpha + 2\alpha\beta) \sum_{i,j,u,v} X_{iv} X_{uj} \partial_{ij} \partial_{uv} \varphi \right. \\ & \left. + (-2\beta + \alpha^2 + \beta^2) \left( \sum_{i,j,u,v} X_{iv} X_{uv} \partial_{ij} \partial_{uj} \varphi \right) \right]. \end{aligned}$$

Substituting  $\alpha = \sqrt{2}/2$  and  $\beta = 1 - \sqrt{2}/2$  we obtain

$$\mathcal{L}\varphi = -\frac{n-1}{2} \sum_{i=1}^n \sum_{j=1}^p X_{ij} \partial_{ij} \varphi + \frac{1}{2} \left[ \sum_{i,j} \partial_{ij}^2 \varphi - \sum_{i,j,u,v} X_{iv} X_{uj} \partial_{ij} \partial_{uv} \varphi \right] = \frac{1}{2} \Delta_{\mathcal{M}_{n,p}} \varphi.$$

□

The next corollary is a direct extension of the above theorem.

COROLLARY 8. *The Fokker-Planck Equation of (11) is given by*

$$(25) \quad \frac{\partial p}{\partial t} = -\nabla_{\mathcal{M}_{n,p}} \cdot (p \nabla_{\mathcal{M}_{n,p}} \mathcal{F}) + \frac{1}{2} \sigma^2(t) \Delta_{\mathcal{M}_{n,p}} p,$$

where  $\nabla_{\mathcal{M}_{n,p}}$ ,  $\nabla_{\mathcal{M}_{n,p}}$ ,  $\Delta_{\mathcal{M}_{n,p}}$  represent the gradient, divergence and Laplace-Beltrami operator on the Stiefel manifold endowed with canonical metric, respectively.

**3. Numerical scheme of the SDE and its convergence.** We next provide a numerical scheme to solve the SDE (11). Our idea is first projecting the random noise in the ambient space to the tangent space of the Stiefel manifold. After that, we apply the Cayley transformation similar as the method discussed in [36]. More precisely, we propose the following update scheme to solve the SDE (11):

$$(26) \quad \begin{cases} Z_k = -\delta_k G_k + \sigma_k (I_n - \beta Y_k Y_k^\top) \delta B_k, \\ A_k = Z_k Y_k^\top - Y_k Z_k^\top, \\ Y_{k+1} = \left( I - \frac{A_k}{2} \right)^{-1} \left( I + \frac{A_k}{2} \right) Y_k. \end{cases}$$

In the case of  $p = n$ , we have a simpler form

$$Z_k = -\delta_k G_k + \alpha \sigma_k \delta B_k.$$

In the spherical constrained case of  $p = 1$ , we can show that

$$A_k = (-\delta_k G_k + \sigma_k \delta B_k) Y_k^\top - Y_k (-\delta_k G_k + \sigma_k \delta B_k)^\top.$$

We point out that there is an efficient way to compute  $Y_{k+1}$  in the case of  $p < n/2$  or  $p = 1$  based on the Sherman-Morrison-Woodbury formula similar to the way discussed in [36].

LEMMA 9 ([36]).

(1) Rewrite  $A_k = U_k V_k^\top$  for  $U_k = [Z_k, Y_k]$  and  $V_k = [Y_k, -Z_k]$ . If  $I - \frac{1}{2} V_k^\top U_k$  is invertible, then

$$(27) \quad Y_{k+1} = Y_k + U_k \left( I - \frac{1}{2} V_k^\top U_k \right)^{-1} V_k^\top Y_k.$$

(2) For the vector case,

(28)

$$Y_{k+1} = Y_k + \frac{Z_k}{1 - (\frac{1}{2})^2(Z_k^\top Y_k)^2 + (\frac{1}{2})^2 Z_k^\top Z_k} - \frac{Z_k^\top Y_k - \frac{1}{2}((Z_k^\top Y_k)^2) + Z_k^\top Z_k}{1 - (\frac{1}{2})^2(Z_k^\top Y_k)^2 + (\frac{1}{2})^2 Z_k^\top Z_k} Y_k.$$

The numerical scheme can now be summarized in [Algorithm 1](#).

---

**Algorithm 1** Numerical Scheme of the SDE

---

**Require:** Diffusion strength  $\sigma(t)$ , time discretization  $t_0 = \tau_0 < \tau_1 < \dots < \tau_K = T$ , initial point  $Y_0 = X(t_0)$ ;

- 1: Let  $\delta_k = \tau_{k+1} - \tau_k$ ,  $\sigma_k = \sigma(\tau_k)$  and  $G_k = \nabla_E \mathcal{F}(Y_k)$  for simplification;
  - 2: Generate a series of  $n$ -by- $p$  independent random matrices  $\{\delta B_k\}_{k=0}^{K-1}$ , the entries of which are independent  $N(0, \delta_k)$  Gaussian variables;
  - 3: **for**  $k = 0 : K - 1$  **do**
  - 4:   Generate  $Y_{k+1}$  from the update scheme (26).
  - 5: **end for**
  - 6: We consider  $Y_k$  to be an appropriate approximation of  $X(\tau_k)$ .
- 

Now we state the strong convergence result. For simplicity, we state and prove the result in the case of constant  $\sigma(t) \equiv \sigma_0$ . Similar result can be proved with variational  $\sigma(t)$  under trivial changes.

**THEOREM 10** (Half Order Strong Convergence). *Denote  $X(T)$  as a solution of the SDE (11) and let  $\delta = \max_k \{\delta_k\}$ . Then there exists a positive constant  $C = C(T)$  independent of  $\delta$ , as well as a constant  $\delta_0 > 0$  such that*

$$(29) \quad \mathbb{E} \|X(T) - Y_K\|_2^2 \leq C\delta, \quad \forall \delta \in (0, \delta_0).$$

*Proof.* Without loss of generality, we suppose  $t_0 = 0$ . For  $0 = t_0 \leq t \leq T$ , we define

$$(30) \quad R(t) := \sup_{0 \leq s \leq t} \mathbb{E} \|X(s) - Y_{k_s}\|_F^2,$$

where  $k_t$  is the largest integer  $k$  for which  $\tau_k$  does not exceed  $t$ , i.e.,

$$k_t := \max\{k = 0, 1, \dots, K : \tau_k \leq t\}.$$

Rewriting (11) into an Ito integral form yields

$$X(s) - X(0) = \int_0^s \left[ -\nabla_{\mathcal{M}} f(X(\tau)) - \frac{n-1}{2} \sigma_0^2 X(\tau) \right] d\tau + \sigma_0 \int_0^s \sum_{u,v} P_{uv}(X(\tau)) dB(\tau).$$

Substituting into (30) and applying the Schwarz inequality yields

$$\begin{aligned}
R(t) &= \sup_{0 \leq s \leq t} \mathbb{E} \left\| \sum_{k=0}^{k_s-1} (Y_{k+1} - Y_k) \right. \\
&\quad \left. + \int_0^s \left[ \nabla_{\mathcal{M}} \mathcal{F}(X(\tau)) + \frac{n-1}{2} \sigma_0^2 X(\tau) \right] d\tau - \sigma_0 \int_0^s P_{X(\tau)}(dB(\tau)) \right\|_F^2 \\
&\leq 7 \sup_{0 \leq s \leq t} \left\{ \mathbb{E} \left\| \sum_{k=0}^{k_s-1} \left[ \mathbb{E}(Y_{k+1} - Y_k | Y_k) - \delta_k \left( -\nabla_{\mathcal{M}} \mathcal{F}(Y_k) - \frac{n-1}{2} \sigma_0^2 Y_k \right) \right] \right\|_F^2 \right. \\
&\quad \left. + \mathbb{E} \left\| \sum_{k=0}^{k_s-1} [Y_{k+1} - Y_k - \mathbb{E}(Y_{k+1} - Y_k | Y_k) - \sigma_0 P_{Y_k}(\delta B_k)] \right\|_F^2 \right. \\
(31) \quad &\quad \left. + \mathbb{E} \left\| \sum_{k=0}^{k_s-1} \left[ \int_{\tau_k}^{\tau_{k+1}} [\nabla_{\mathcal{M}} \mathcal{F}(X(\tau))] d\tau - \delta_k \nabla_{\mathcal{M}} \mathcal{F}(Y_{\tau_k}) \right] \right\|_F^2 \right. \\
&\quad \left. + \mathbb{E} \left\| \sum_{k=0}^{k_s-1} \left[ \int_{\tau_k}^{\tau_{k+1}} \left( \frac{n-1}{2} \sigma_0^2 X(\tau) \right) d\tau - \delta_k \left( \frac{n-1}{2} \sigma_0^2 Y_{\tau_k} \right) \right] \right\|_F^2 \right. \\
&\quad \left. + \mathbb{E} \left\| \sigma_0 \sum_{k=0}^{k_s-1} \left[ \int_{\tau_k}^{\tau_{k+1}} P_{X(\tau)}(dB(\tau)) - P_{Y_k}(\delta B_k) \right] \right\|_F^2 \right. \\
&\quad \left. + \mathbb{E} \left\| \int_{\tau_{k_s}}^s \left( \nabla_{\mathcal{M}} \mathcal{F}(X(\tau)) + \frac{n-1}{2} \sigma_0^2 X(\tau) \right) d\tau \right\|_F^2 \right. \\
&\quad \left. + \mathbb{E} \left\| \sigma_0 \int_{\tau_{k_s}}^s P_{X(\tau)}(dB(\tau)) \right\|_F^2 \right\}
\end{aligned}$$

We next analyze the seven terms of (31) in order. Iterating (26) repeatedly yields

$$(32) \quad Y_{k+1} - Y_k = A_k Y_k + \frac{1}{2} A_k^2 Y_k + \frac{1}{8} A_k^3 (Y_k + Y_{k+1}).$$

Direct calculus shows that

$$\begin{aligned}
(33) \quad A_k Y_k &= Z_k - Y_k Z_k^\top Y_k \\
&= -\delta_k (G_k - Y_k G_k^\top Y_k) + \sigma_0 [(I - \beta Y_k Y_k^\top) \delta B_k - Y_k \delta B_k^\top (I - \beta Y_k Y_k^\top) Y_k] \\
&= -\delta_k (\nabla_{\mathcal{M}} \mathcal{F}(Y_k)) + \sigma_0 (\delta B_k - \alpha Y_k \delta B_k^\top Y_k - \beta Y_k Y_k^\top \delta B_k) \\
&= -\delta_k (\nabla_{\mathcal{M}} \mathcal{F}(Y_k)) + \sigma_0 P_{Y_k}(\delta B_k),
\end{aligned}$$

and

$$\begin{aligned}
(34) \quad A_k^2 Y_k &= (Z_k Y_k^\top - Y_k Z_k^\top) A_k Y_k \\
&= [\delta_k (-G_k Y_k^\top + Y_k G_k^\top) + \sigma_0 ((I - \beta Y_k Y_k^\top) \delta B_k Y_k^\top - Y_k \delta B_k^\top (I - \beta Y_k Y_k^\top))] \\
&\quad \cdot [-\delta_k \nabla_{\mathcal{M}} \mathcal{F}(Y_k) + \sigma_0 P_{Y_k}(\delta B_k)].
\end{aligned}$$

We claim that

$$(35) \quad \mathbb{E}\{[(I - \beta Y_k Y_k^\top) \delta B_k Y_k^\top - Y_k \delta B_k^\top (I - \beta Y_k Y_k^\top)](P_{Y_k}(\delta B_k)) | Y_k\} = -(n-1) \delta_k Y_k.$$

In fact, we can show that

$$(36) \quad \begin{aligned} & \mathbb{E}\{[(I - \beta Y_k Y_k^\top) \delta B_k Y_k^\top - Y_k \delta B_k^\top (I - \beta Y_k Y_k^\top)](P_{Y_k}(\delta B_k)) | Y_k\} \\ &= \mathbb{E}\{(\delta B_k Y_k^\top - \beta Y_k Y_k^\top \delta B_k Y_k^\top - Y_k \delta B_k^\top + \beta Y_k \delta B_k^\top Y_k Y_k^\top) \\ & \quad \cdot (\delta B_k - \alpha Y_k \delta B_k^\top Y_k - \beta Y_k Y_k^\top \delta B_k) | Y_k\}. \end{aligned}$$

Let  $Q_k = [Y_k, Y_k^\perp]$  and  $N_k = Q_k^\top \delta B_k$ , and one can show that the entries of  $N_k$  are independent  $N(0, \delta_k)$  variables. By substituting  $\delta B_k = Q_k N_k$  back into the above equation and expanding the corresponding terms, we have

$$\begin{aligned} \mathbb{E}\{Q_k N_k Y_k^\top Q_k N_k | Y_k\} &= \mathbb{E}\{Q_k N_k [I_p, 0] N_k | Y_k\} = \delta_k Q_k \begin{pmatrix} I_p \\ 0 \end{pmatrix} = \delta_k Y_k, \\ -\alpha \mathbb{E}\{Q_k N_k Y_k^\top Y_k N_k^\top Q_k^\top Y_k | Y_k\} &= -\delta_k \alpha p Q_k I_n Q_k^\top Y_k = -\delta_k \alpha p Y_k, \\ -\beta \mathbb{E}\{Q_k N_k Y_k^\top Y_k Y_k^\top Q_k N_k | Y_k\} &= -\beta \mathbb{E}\{Q_k N_k I_p [I_p, 0] N_k | Y_k\} = -\delta_k \beta Y_k, \\ -\beta \mathbb{E}\{Y_k Y_k^\top Q_k N_k Y_k^\top Q_k N_k | Y_k\} &= -\beta \mathbb{E}\{Y_k [I_p, 0] N_k [I_p, 0] N_k | Y_k\} = -\delta_k \beta Y_k, \\ \alpha \beta \mathbb{E}\{Y_k Y_k^\top Q_k N_k Y_k^\top Y_k N_k^\top Q_k^\top Y_k | Y_k\} &= \alpha \beta \mathbb{E}\{Y_k [I_p, 0] N_k N_k^\top \begin{pmatrix} I_p \\ 0 \end{pmatrix} | Y_k\} = \delta_k \alpha \beta p Y_k, \\ \beta^2 \mathbb{E}\{Y_k Y_k^\top Q_k N_k Y_k^\top Y_k Y_k^\top Q_k N_k | Y_k\} &= \beta^2 \mathbb{E}\{Y_k [I_p, 0] N_k [I_p, 0] N_k | Y_k\} = \delta_k \beta^2 Y_k, \\ & \quad -\mathbb{E}\{Y_k N_k^\top Q_k^\top Q_k N_k | Y_k\} = -\delta_k n Y_k, \\ \alpha \mathbb{E}\{Y_k N_k^\top Q_k^\top Y_k N_k^\top Q_k^\top Y_k | Y_k\} &= \alpha \mathbb{E}\{Y_k N_k^\top \begin{pmatrix} I_p \\ 0 \end{pmatrix} N_k^\top \begin{pmatrix} I_p \\ 0 \end{pmatrix} | Y_k\} = \delta_k \alpha Y_k, \\ \beta \mathbb{E}\{Y_k N_k^\top Q_k^\top Y_k Y_k^\top Q_k N_k | Y_k\} &= \beta \mathbb{E}\{Y_k N_k^\top \text{diag}\{I_p, 0_{n-p}\} N_k | Y_k\} = \delta_k \beta p Y_k, \text{ (twice),} \\ & \quad -\alpha \beta \mathbb{E}\{Y_k N_k^\top Q_k^\top Y_k Y_k^\top Y_k N_k^\top Q_k^\top Y_k | Y_k\} \\ &= -\alpha \beta \mathbb{E}\{Y_k N_k^\top \begin{pmatrix} I_p \\ 0 \end{pmatrix} N_k^\top \begin{pmatrix} I_p \\ 0 \end{pmatrix} | Y_k\} = -\delta_k \alpha \beta Y_k, \\ & \quad -\beta^2 \mathbb{E}\{Y_k N_k^\top Q_k^\top Y_k Y_k^\top Y_k Y_k^\top Q_k N_k | Y_k\} \\ &= -\beta^2 \mathbb{E}\{Y_k N_k^\top \text{diag}\{I_p, 0_{n-p}\} N_k | Y_k\} = -\delta_k \beta^2 p Y_k. \end{aligned}$$

Taking sum of the above terms yields (35). A direct corollary of (35) is

$$(37) \quad \mathbb{E} \left\| \mathbb{E}(Y_{k+1} - Y_k | Y_k) - \delta_k \left( -\nabla_{\mathcal{M}} \mathcal{F}(Y_k) - \frac{n-1}{2} \sigma_0^2 Y_k \right) \right\|_F^2 \leq C_1' \delta_k^3.$$

Hence, we can derive an estimation of the first term in (31) as

$$(38) \quad \begin{aligned} & \mathbb{E} \left\| \sum_{k=0}^{k_s-1} \left[ \mathbb{E}(Y_{k+1} - Y_k | Y_k) - \delta_k \left( -\nabla_{\mathcal{M}} \mathcal{F}(Y_k) - \frac{n-1}{2} \sigma_0^2 Y_k \right) \right] \right\|_F^2 \\ & \leq \delta \left( \sum_{k=0}^{k_s-1} \delta_k \right) \sum_{k=0}^{k_s-1} \frac{1}{\delta_k^2} \mathbb{E} \left\| \mathbb{E}(Y_{k+1} - Y_k | Y_k) - \delta_k \left( -\nabla_{\mathcal{M}} \mathcal{F}(Y_k) - \frac{n-1}{2} \sigma_0^2 Y_k \right) \right\|_F^2 \\ & \leq \delta \left( \sum_{k=0}^{k_s-1} \delta_k \right) \left( \sum_{k=0}^{k_s-1} C_1' \delta_k \right) \leq C_1 \delta. \end{aligned}$$

The first inequality of (38) is due to Cauchy-Schwartz inequality and  $\delta = \max\{\delta_k\}$ .

The second term of (31) can be evaluated in view that all the cross-product terms vanish under the Frobenius norm:

$$\begin{aligned}
(39) \quad & \mathbb{E} \left\| \sum_{k=0}^{k_s-1} [Y_{k+1} - Y_k - \mathbb{E}(Y_{k+1} - Y_k | Y_k) - \sigma_0 P_{Y_k}(\delta B_k)] \right\|_F^2 \\
&= \sum_{k=0}^{k_s-1} \mathbb{E} \left\| [Y_{k+1} - Y_k - \mathbb{E}(Y_{k+1} - Y_k | Y_k) - \sigma_0 P_{Y_k}(\delta B_k)] \right\|_F^2 \\
&\leq \sum_{k=0}^{k_s-1} (\mathbb{E} \|A_k Y_k - \sigma_0 P_{Y_k}(\delta B_k)\|_F^2 + C'_2 \delta_k^2) \\
&\leq \sum_{k=0}^{k_s-1} C_2 \delta_k^2 \leq C_2 \delta.
\end{aligned}$$

The third term of (31) can be estimated in view of the smoothness of  $\nabla_{\mathcal{M}} \mathcal{F}$ :

$$\begin{aligned}
(40) \quad & \mathbb{E} \left\| \sum_{k=0}^{k_s-1} \left[ \int_{\tau_k}^{\tau_{k+1}} [-\nabla_{\mathcal{M}} \mathcal{F}(X(\tau))] d\tau + \delta_k \nabla_{\mathcal{M}} \mathcal{F}(Y_{k_\tau}) \right] \right\|_F^2 \\
&= \mathbb{E} \left\| \int_0^{\tau_{k_s}} [\nabla_{\mathcal{M}} \mathcal{F}(Y_{k_\tau}) - \nabla_{\mathcal{M}} \mathcal{F}(X(\tau))] d\tau \right\|_F^2 \\
&\leq T \int_0^{\tau_{k_s}} \mathbb{E} \left\| \nabla_{\mathcal{M}} \mathcal{F}(Y_{k_\tau}) - \nabla_{\mathcal{M}} \mathcal{F}(X(\tau)) \right\|_F^2 d\tau \\
&\leq TC'_3 \int_0^{\tau_{k_s}} \mathbb{E} \|X(\tau) - Y_{k_\tau}\|_F^2 d\tau \\
&= TC'_3 \int_0^{\tau_{k_s}} R(\tau) d\tau \leq TC'_3 \int_0^t R(\tau) d\tau := C_3 \int_0^t R(\tau) d\tau.
\end{aligned}$$

Similarly one can show that the forth term of (31) can be bounded by

$$(41) \quad \mathbb{E} \left\| \sum_{k=0}^{k_s-1} \left[ \int_{\tau_k}^{\tau_{k+1}} \left( \frac{n-1}{2} \sigma_0^2 X(\tau) \right) d\tau - \delta_k \left( \frac{n-1}{2} \sigma_0^2 Y_{k_\tau} \right) \right] \right\|_F^2 \leq C_4 \int_0^t R(\tau) d\tau.$$

The fifth term of (31) can be estimated using Ito's isometry and the smoothness of  $P_{uv}$ :

$$\begin{aligned}
(42) \quad & \mathbb{E} \left\| \sigma_0 \sum_{k=0}^{k_s-1} \left[ \int_{\tau_k}^{\tau_{k+1}} P_{X(\tau)}(dB(\tau)) - P_{Y_k}(\delta B_k) \right] \right\|_F^2 \\
&= \sigma_0^2 \mathbb{E} \left\| \sum_{u,v} \int_0^{\tau_{k_s}} [P_{uv}(X(\tau) - P_{uv}(Y_{k_\tau}))] dB_{uv}(\tau) \right\|_F^2 \\
&= \sigma_0^2 \sum_{u,v} \int_0^{\tau_{k_s}} \mathbb{E} \|P_{uv}(X_\tau) - P_{uv}(Y_{k_\tau})\|_F^2 d\tau \\
&\leq C_5 \int_0^{\tau_{k_s}} \mathbb{E} \|X(\tau) - Y_{k_\tau}\|_F^2 d\tau = C_5 \int_0^{\tau_{k_s}} R(\tau) d\tau \leq C_5 \int_0^t R(\tau) d\tau.
\end{aligned}$$

The last two terms can be estimated as

$$(43) \quad \mathbb{E} \left\| \int_{\tau_{k_s}}^s \left( -\nabla_{\mathcal{M}} \mathcal{F}(X(\tau)) - \frac{n-1}{2} \sigma_0^2 X(\tau) \right) d\tau \right\|_F^2 \leq C_6 \delta^2.$$

and

$$(44) \quad \mathbb{E} \left\| \sigma_0 \int_{\tau_{k_s}}^s P_{X(\tau)}(dB(\tau)) \right\|_F^2 \leq C_7 \delta.$$

Taking the above estimation together yields

$$(45) \quad R(t) \leq 7 \left[ (C_1 + C_2 + C_7) \delta + C_6 \delta^2 + (C_3 + C_4 + C_5) \int_0^t R(\tau) d\tau \right].$$

It follows directly from the Gronwall inequality that

$$(46) \quad R(t) \leq C \delta, \quad \delta \in (0, \delta_0),$$

where  $C$  is A constant independent of  $\delta$  and  $\delta_0 > 0$ .  $\square$

**4. IDDM Algorithm and Global convergence Analysis.** Now we can generalize existing methods based on diffusion equation (9) to the Stiefel Manifold. The method we use in the following is a generalization of Intermittent Diffusion (ID) [7], namely Intermittent Diminishing Diffusion on Stiefel Manifold (IDDM), in which the diffusion strength is diminishing in every single cycle.

---

**Algorithm 2** Intermittent Diminishing Diffusion on Stiefel Manifold (IDDM)

---

**Require:** Maximum number of cycles  $N$ , diffusion strength  $\sigma_n$ , diffusion time (in one cycle)  $T_n$ , initial point  $X_0$  (usually random selected);

- 1:  $X_{\text{opt}} \leftarrow X_0, k \leftarrow 0$ ;
  - 2: **while** Terminal conditions not satisfied **do**
  - 3:   **if**  $k \geq N$  **then**
  - 4:     **break**
  - 5:   **end if**
  - 6:   Numerically solve (11) by Algorithm 1 starting from  $X_k$  using time  $T_k$  and diffusion strength  $\sigma(t) = \sigma_k$  to obtain  $X'_{k+1}$ ;
  - 7:   Solve  $dX_t = -\nabla_{\mathcal{M}} \mathcal{F}(X_t) dt$  by local algorithm starting from  $X'_{k+1}$  until convergence and get  $X_{k+1}$ ;
  - 8:   **if**  $f(X_{k+1}) < f(X_{\text{opt}})$  **then**
  - 9:      $X_{\text{opt}} \leftarrow X_{k+1}$ ;
  - 10:   **end if**
  - 11:    $k \leftarrow k + 1$ ;
  - 12: **end while**
- 

We first notice that the method can also be viewed as selecting

$$(47) \quad \sigma(t) = \sum_{i=1}^N \sigma_i I_{[S_i, S_i+T_i]}(t),$$

where  $S_i$  is the starting time of each piece.

To provide the convergence results, we will first give some analysis for the Fokker-Planck Equation (25). The classic results yield the next theorem.

**THEOREM 11.** *Assume that  $\sigma(t) = \sigma_0$  is a constant. The distribution  $p(x, t)$  converges ( $\ell_1$ ) to the Gibbs distribution*

$$(48) \quad \tilde{p}_{\sigma_0}(x) = \frac{1}{Z} e^{-2\mathcal{F}/\sigma_0^2},$$

where  $Z$  is the normalization constant  $Z = \int_{\mathcal{M}} e^{-2\mathcal{F}/\sigma_0^2}$ .

*Proof.* To simplify the problem, we set  $\sigma_0 = \sqrt{2}$  or let  $t' \leftarrow 2t/\sigma_0^2$  and  $\mathcal{F}' \leftarrow 2\mathcal{F}/\sigma_0^2$  to transfer the Fokker-Planck equation to one with  $\sigma_0 = \sqrt{2}$ . Define the relative entropy

$$(49) \quad H(p|q) = \int_{\mathcal{M}} p \log\left(\frac{p}{q}\right) dx,$$

for any two probability density function  $p, q$  (on the manifold). The Csiszár-Kullback inequality shows that

$$(50) \quad \|p - q\|_{\ell_1}^2 \leq 2H(p|q).$$

The canonical Stiefel manifold is known as Einstein manifold in the case of  $n = p$  and thus the Ricci curvature is positive definite [25].

For general canonical stiefel manifolds, the same results are shown in [13]. It is given in [21, 34] that  $\mathcal{F}_0(X) = 0$  satisfies a logarithmic Sobolev inequality with constant  $\lambda_0$  which is the smallest eigenvalue of the Ricci curvature. It follows from [21, 34] that  $\mathcal{F}(X)$  also satisfies a logarithmic Sobolev inequality with constant  $\lambda = \lambda_0(\max_{\mathcal{F}} - \min_{\mathcal{F}})$ , which indicates that

$$(51) \quad H(p(\cdot, t)|\tilde{p}_{\sigma_0}) \leq e^{-2\lambda t} H(p(\cdot, 0)|\tilde{p}_{\sigma_0}).$$

From the above analysis, we have

$$(52) \quad \|p(\cdot, t) - \tilde{p}_{\sigma_0}\|_{\ell_1}^2 \leq 2e^{-2\lambda t} H(p(\cdot, 0)|\tilde{p}_{\sigma_0}),$$

which completes the proof.  $\square$

We next provide the convergence results of [Algorithm 2](#), which is nearly the same to the proof in [7] in the Euclidean space.

**THEOREM 12** (Convergence of [Algorithm 2](#)). *Assume that the local algorithm satisfies  $\mathcal{F}(X_k) \leq \mathcal{F}(X'_k)$ . Let the set of global minimizers be  $P$ , the global minimum be  $\mathcal{F}^*$ , and  $X_{opt}$  to be the optimal solution obtained by [Algorithm 2](#). For any given  $\epsilon > 0$  and  $\zeta > 0$ , let  $U$  be the basin of global minima, i.e.,  $U = \{X \in \mathcal{M}_{n,p} \mid \mathcal{F}(X) < \mathcal{F}^* + \zeta\}$ . Then the following two statements hold:*

1.  $\forall \eta \in (0, 1)$ ,  $\exists \sigma > 0$  and  $T > 0$  (as a function of  $\sigma$ ) such that if  $\sigma_i \leq \sigma$  and  $T_i > T(\sigma_i)$ , then  $\mathbb{P}(X'_i \in U) \geq \eta$ .
2. The probability to reach  $U$  after  $N$  cycles is at least  $1 - (1 - \eta)^N$ , namely,  $\mathbb{P}(\exists i, X'_i \in U) > 1 - (1 - \eta)^N$ . Thus, there exists  $N_0 > 0$  such that if  $\sigma_i \leq \sigma$ ,  $T_i > T(\sigma_i)$  and  $N > N_0$ ,

$$(53) \quad \mathbb{P}(\mathcal{F}(X_{opt}) < \mathcal{F}^* + \zeta) \geq 1 - \epsilon.$$

*Proof.* A small neighborhood  $U$  can be given so that  $\forall X \in U$ ,  $\mathcal{F}(X) < \mathcal{F}^* + \zeta$ . We only need to prove that  $\mathbb{P}(\exists k, \text{ s.t. } X'_k \in U) \geq 1 - \epsilon$ .



From (48),  $\forall \eta \in (0, 1)$ ,  $\exists \sigma > 0$  such that if  $\sigma_i \leq \sigma$ ,

$$(54) \quad \int_U \tilde{p}_{\sigma_i}(x) dx > \eta + (1 - \eta)/2.$$

Meanwhile, Theorem 11 yields that  $\exists T > 0$  such that if  $T_i > T$ ,

$$(55) \quad \|p(\cdot, S_i + T_i) - \tilde{p}_{\sigma_i}\|_{\ell_1} < (1 - \eta)/2.$$

Hence, we have

$$(56) \quad \mathbb{P}(X'_i \in U) = \int_U \tilde{p}_{\sigma_i} dx - \int_U \tilde{p}_{\sigma_i} - p(x, S_i + T_i) dx \geq \eta.$$

Independent intervals yields that

$$(57) \quad \mathbb{P}(\forall i, X'_i \in U^c) < (1 - \eta)^N.$$

Select a proper  $N_0$  such that  $(1 - \eta)^{N_0} \leq \epsilon$  and we complete the proof.  $\square$

REMARK 13. The results of Theorem 12 can be improved if we impose some stronger conditions on the object function and the local algorithm. If 1) the local algorithm always achieve a nearest local minimizer and 2) there are finite local minimizers (which is acceptable for a compact set), then the results can be improved as  $\mathbb{P}(\text{dist}(X_{opt}, P) < \zeta) \geq 1 - \epsilon$ . The proof is the same as [7].

REMARK 14. We have provided some analysis for the piecewise constant  $\sigma(t)$  proposed by [7]. Notice that other  $\sigma(t)$  may also give global convergence. For example, one can apply the  $\sigma(t) = c/\sqrt{\log(t+2)}$  given by CDD and the proof of convergence is the same. One can refer to [6, 9] for the proof.

**5. Numerical Experiments.** In this section, we demonstrate the effectiveness of IDD methods on Stiefel Manifold (IDDM) on a variety of test problems. The first two subsections are devoted to the spherically constrained problems, while the last one focuses on the orthogonality constrained problem. We should point out that we have also test many problems, such as conformal mapping [12, 15], p-Harmonic flow [17, 32, 33, 11], compressed modes [26] and nonlinear eigenvalue problem in density functional theory [19, 35]. They are not chosen in this section because the local algorithm is often able to return a pretty solution (or even “global solution”) in a single run.

The performance of IDDM is mainly compared with the *Random-Start* local method dubbed as RSlocal, which randomly selects an initial point and then performs the local algorithm. The local algorithm that we employ is the curvilinear search method with Barzilai-Borwein steps (Algorithm 2 in [36]). Each run of IDDM consists of ten cycles while RSlocal is made up of ten trials of the local algorithm starting from randomly generated points. The parameter  $\sigma_i$  in (47) is set to  $\sigma_i = \alpha/(id_t)^{1/2(n-1)}$ , where  $d_t$  is the step length,  $n$  is the dimension of the variables and  $\alpha$  is the initial diffusion strength. All experiments were performed on a workstation with an Intel Xeon E5-2640 v3 2.60GHz processor with access to 64 GB of RAM.

**5.1. Homogeneous Polynomial Optimization.** In this subsection, we evaluate the performance on homogeneous polynomial problems. The test polynomial is selected from [36] which cannot be globally minimized effectively by the local methods:

$$(58) \quad \min_{x \in \mathbb{R}^n} \mathcal{F}(x) = \sum_{1 \leq i \leq n} x_i^6 + \sum_{1 \leq i \leq n-1} x_i^3 x_{i+1}^3, \quad \text{s.t.} \quad \|x\|_2 = 1.$$

For each of  $n = 10, 20, \dots, 200$ , we repeat 50 independent runs of IDDM and RSlocal. The initial diffusion strength  $\alpha$  is selected as  $1/n$ . The minimum, mean and maximum of the objective function values, as well as the averaged cpu time in seconds are reported in Table 1. The corresponding mean and min are further illustrated in the left side of Figure 1. Our numerical results indicate that IDDM are always much better than RSlocal in this problem.

We further numerically explore the dependency of the performance of IDDM to the diffusion strength  $\alpha$ . For each  $n$  ranging from 40 to 200, we repeat 50 independent tests of RSlocal and denote the averaged objective function values as  $\mathcal{F}_{\text{RSlocal}}$ . Similarly, we repeat 50 runs of IDDM with different initial diffusion strengths  $\sigma$  from  $10^{-4}$  to  $10^0$  and the averaged objective function values are denoted by  $\mathcal{F}_{\text{IDDM}}$ . Each pixel in the right side of Figure 1 is a value of  $-\log_{10}(\mathcal{F}_{\text{IDDM}}/\mathcal{F}_{\text{RSlocal}})$ . A positive value indicates an improvement achieved by IDDM over RSlocal while a negative value means that IDDM is worse than RSlocal. This image clearly shows that our IDDM outperforms RSlocal with the right choice of the diffusion strength illustrated in the region with the red color.

TABLE 1  
Numerical results of polynomial optimization (58)

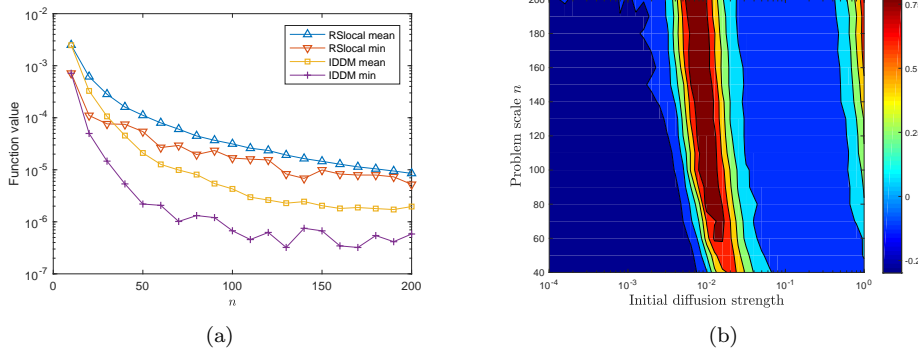
$n$	RSlocal				IDDM			
	min	mean	max	cpu (s)	min	mean	max	cpu (s)
10	7.2e-04	2.5e-03	6.3e-03	0.041	7.2e-04	2.5e-03	4.8e-03	0.044
20	1.1e-04	6.1e-04	1.3e-03	0.047	5.0e-05	3.3e-04	1.1e-03	0.087
30	7.6e-05	2.8e-04	4.8e-04	0.057	1.5e-05	1.1e-04	2.5e-04	0.116
40	7.5e-05	1.6e-04	2.5e-04	0.065	5.4e-06	4.5e-05	1.2e-04	0.129
50	5.4e-05	1.1e-04	1.7e-04	0.078	2.2e-06	2.1e-05	5.5e-05	0.166
60	2.7e-05	8.0e-05	1.4e-04	0.087	2.1e-06	1.3e-05	3.5e-05	0.154
70	2.9e-05	6.0e-05	9.0e-05	0.100	1.0e-06	9.9e-06	2.6e-05	0.173
80	2.0e-05	4.5e-05	6.3e-05	0.095	1.3e-06	8.1e-06	4.2e-05	0.153
90	2.3e-05	3.7e-05	5.3e-05	0.099	1.2e-06	5.4e-06	1.7e-05	0.169
100	1.7e-05	3.1e-05	4.5e-05	0.104	6.7e-07	4.3e-06	1.4e-05	0.175
110	1.6e-05	2.6e-05	3.6e-05	0.118	4.6e-07	3.0e-06	8.6e-06	0.166
120	1.5e-05	2.3e-05	3.1e-05	0.115	6.2e-07	2.6e-06	8.9e-06	0.174
130	8.3e-06	1.9e-05	2.5e-05	0.125	3.2e-07	2.3e-06	4.6e-06	0.191
140	6.8e-06	1.6e-05	2.1e-05	0.128	7.5e-07	2.4e-06	7.3e-06	0.172
150	9.9e-06	1.5e-05	2.1e-05	0.136	6.7e-07	2.0e-06	6.9e-06	0.180
160	8.3e-06	1.3e-05	1.8e-05	0.140	3.4e-07	1.8e-06	7.5e-06	0.184
170	7.9e-06	1.1e-05	1.4e-05	0.153	3.2e-07	1.9e-06	5.0e-06	0.183
180	7.9e-06	1.0e-05	1.3e-05	0.152	5.4e-07	1.8e-06	5.0e-06	0.186
190	7.3e-06	9.5e-06	1.2e-05	0.154	4.1e-07	1.7e-06	3.4e-06	0.190
200	5.2e-06	8.5e-06	1.1e-05	0.160	5.8e-07	2.0e-06	7.0e-06	0.189

**5.2. Biquadratic optimization.** We next consider the so-called biquadratic optimization over unit spheres [18]:

$$(59) \quad \begin{aligned} \min_{x \in \mathbb{R}^n, y \in \mathbb{R}^n} b(x, y) &= \sum_{1 \leq i, k \leq n, 1 \leq j, l \leq n} b_{ijkl} x_i y_j x_k y_l \\ \text{s.t. } \|x\| &= 1, \|y\| = 1. \end{aligned}$$

Without loss of generality, we impose the symmetric property  $b_{ijkl} = b_{kjil} = b_{ilkj}$  for  $i, k, j, l = 1, \dots, n$ . A semidefinite programming relaxation approach is proposed in [18]. Since Examples 5.1 to 5.3 in this reference can be easily found by local solvers, we generate the coefficients  $b_{ijkl}$  as following:

FIG. 1. (a) The objective function values of IDDM and RSlocal on (58). (b)  $-\log_{10}(\mathcal{F}_{\text{IDDM}}/\mathcal{F}_{\text{RSlocal}})$ , i.e., the performance of IDDM using various initial diffusion strength with respect to RSlocal.



case i)  $b_{ijkl} = (-1)^{i+j+k+l}|c|$ , where  $c$  is a Gaussian random variable.  
 case ii)  $b_{ijkl} = |c_1|1_{c_2 > \eta}$ , where  $c_1$  is a Gaussian random variable,  $c_2$  is uniformly distributed in  $[0, 1]$  and  $\eta \in (0, 1)$ .

For each of  $n = 6, 7, \dots, 25$ , we repeat 50 independent runs of IDDM and RSlocal. For the parameter  $\alpha$  of IDDM, we select a few values in  $[10^{-4}, 10^2]$  for each  $n$  and choose the one with the best performance. The minimum, mean and maximum of the difference between the objective function values and the smallest objective function value identified in the 50 runs are reported in Tables 2 and 3. From the tables, we can see that both IDDM and RSlocal can find the “smallest” function values. IDDM usually performs better than RSlocal in most cases in terms of the mean value.

TABLE 2  
 Numerical results of biquadratic optimization: case i

$n$	RSlocal				IDDM			
	min	mean	max	cpu (s)	min	mean	max	cpu (s)
6	5.2e-14	1.4e-02	2.5e-01	0.033	1.5e-14	8.3e-03	1.8e-02	0.034
7	3.6e-14	2.2e-02	2.8e-01	0.020	3.7e-14	1.4e-02	2.8e-01	0.030
8	4.8e-14	1.1e-01	1.6e+00	0.026	2.7e-15	2.5e-13	7.1e-13	0.030
9	2.5e-14	1.4e-01	3.9e-01	0.032	2.2e-14	4.3e-12	2.6e-11	0.037
10	3.3e-14	1.1e-01	1.2e+00	0.041	7.1e-15	3.4e-12	1.9e-11	0.046
11	2.7e-14	8.0e-02	6.4e-01	0.046	2.8e-14	1.6e-11	1.8e-10	0.054
12	9.9e-14	3.5e-02	2.1e-01	0.056	1.4e-13	1.9e-02	1.6e-01	0.075
13	3.7e-14	2.5e-01	7.7e-01	0.059	2.0e-14	2.0e-01	7.7e-01	0.076
14	1.1e-13	2.4e-01	1.1e+00	0.073	8.2e-14	1.4e-01	9.0e-01	0.102
15	1.2e-13	1.3e-01	5.2e-01	0.085	1.2e-13	4.8e-12	6.4e-11	0.088
16	5.0e-13	5.2e-02	4.6e-01	0.110	2.4e-12	2.7e-02	3.1e-01	0.163
17	1.4e-14	6.5e-01	1.5e+00	0.112	3.0e-13	3.9e-12	6.2e-11	0.111
18	2.0e-13	1.9e-01	9.5e-01	0.136	6.6e-14	6.1e-02	4.6e-01	0.187
19	2.9e-13	3.6e-01	9.5e-01	0.186	1.4e-14	2.5e-12	1.9e-11	0.178
20	4.1e-14	4.0e-01	1.3e+00	0.225	2.8e-13	2.3e-01	9.8e-01	0.335
21	4.3e-14	4.9e-01	1.2e+00	0.267	4.4e-14	3.0e-01	8.7e-01	0.409
22	3.3e-13	4.2e-01	1.0e+00	0.324	4.4e-13	2.9e-11	1.4e-10	0.472
23	1.0e-13	6.9e-01	1.8e+00	0.410	2.7e-13	6.7e-12	2.5e-11	0.454
24	1.2e-13	4.7e-01	1.1e+00	0.484	1.2e-12	3.4e-01	9.9e-01	0.711
25	5.6e-13	3.4e-01	1.1e+00	0.556	5.1e-13	3.1e-01	1.2e+00	0.876

We next demonstrate the performance of IDDM with respect to the initial diffusion strength  $\alpha$ . For each  $n = \{18, 20\}$ , we repeat 50 independent tests of RSlocal. The averaged difference to global objective function values is plotted as the red line in Figure 2. Then we repeat 50 runs of IDDM with different initial diffusion strengths  $\sigma$  from  $10^{-4}$  to  $10^2$ . The averaged difference to global objective function values are depicted as the blue curve in Figure 2. We can see that our IDDM outperforms RSlocal if the diffusion strength is chosen suitably. Similar behavior can be observed on other dimensions of  $n$ .

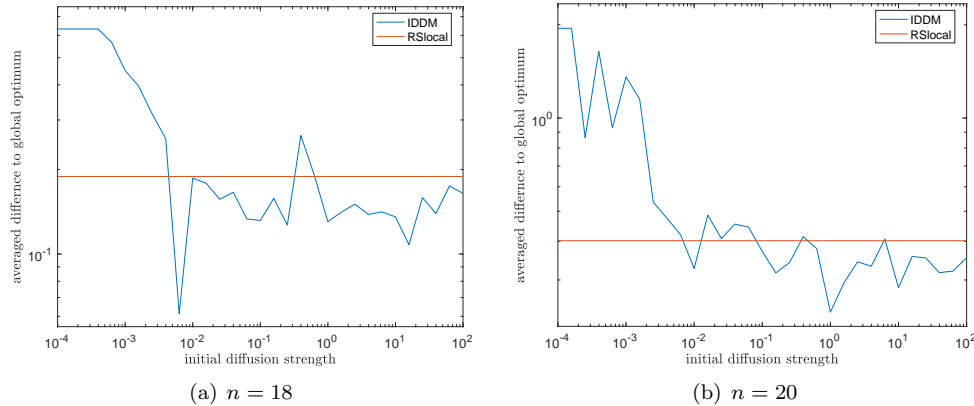


FIG. 2. The performance of IDDM with respect to the initial diffusion strength

**5.3. Computation of Stability Number.** Let  $G = (V, E)$  be an undirected graph. A stable (independent) set in  $G$  is a set of vertices that are mutually non-adjacent. The *stability number*  $S(G)$  for a given graph  $G$  is defined as the size of a maximum stable set in  $G$ . It was shown by Motzkin and Straus [22] that

$$S(G)^{-1} = \min_{\|x\|_2=1} \sum_{i=1}^n x_i^4 + 2 \sum_{(i,j) \in E} x_i^2 x_j^2,$$

which is a single spherically constrained problem. We select a few typical graphs as in [36] and we repeat 50 independent runs of IDDM and RSlocal. The parameter  $\alpha$  is set to 0.005 in IDDM. The size  $|V|$  of the graph, the mean and maximum of  $S(G)$  as well as the cpu time are presented in Table 4. Note that the larger the value  $S(G)$  is obtained, the better the stability number is estimated. We can see that IDDM almost always achieve a better solution than RSlocal.

**5.4. Structure Determination in Cryo-EM.** We now consider an example with multiple orthogonality constraints that arises from Cryo-EM [31]. In this test problem, we try to recover  $N$  orientations  $\{\tilde{R}_i\}$  from two dimensional (2D) projection images  $\{P_i\}$  of a three dimensional (3D) object. Each  $\tilde{R}_i \in \mathbb{R}^{3 \times 3}$  describes a 3D orthogonal matrix or rotation, i.e.,  $\tilde{R}_i^\top \tilde{R}_i = I_3$  and  $\det(\tilde{R}_i) = 1$ . Let  $\tilde{c}_{ij} = (x_{ij}, y_{ij}, 0)$  be the common line of the Fourier transforms of  $P_i$  and  $P_j$  (viewed in  $P_i$ ). When the data are exact, it follows from the Fourier projection-slice theorem [31] that the common lines must coincide, i.e.,

$$\tilde{R}_i \tilde{c}_{ij} = \tilde{R}_j \tilde{c}_{ji}.$$

Since the third column  $\tilde{R}_i^3$  can be recovered from the first two columns  $\tilde{R}_i^1$  and  $\tilde{R}_i^2$  as  $\tilde{R}_i^3 = \pm \tilde{R}_i^1 \times \tilde{R}_i^2$ , the rotations  $\{\tilde{R}_i\}$  can be compressed to  $3 \times 2$  matrix. Therefore, the corresponding optimization problem can be formulated as

$$(60) \quad \min_{R_i} \sum_{i=1}^N \rho(R_i c_{ij}, R_j c_{ji}), \quad \text{s.t.} \quad R_i^\top R_i = I_2, R_i \in \mathbb{R}^{3 \times 2}$$

where  $\rho$  is the function representing the distance between the two vectors,  $R_i$  is made up of the first two columns of  $\tilde{R}_i$  and  $c_{ij}$  consists of the first two elements of  $\tilde{c}_{ij}$ . The distance function  $\rho(u, v) = \|u - v\|_2$  is chosen in [31] and it leads to an eigenvector relaxation and semidefinite programming relaxation. In our experiments, we select  $\rho(u, v) = \|u - v\|_q$  with  $q = 0.5$  since it often leads to better mean square error defined as follows. Note that it holds  $O\tilde{R}_i\tilde{c}_{ij} = O\tilde{R}_j\tilde{c}_{ji}$  for any fixed orthogonal matrix  $O \in \mathbb{R}^{3 \times 3}$ . Hence, we measure the error between the recovered rotations  $\hat{R}_i$  and real rotations  $\tilde{R}_i$  by the mean square error (MSE) defined as

$$\text{MSE} = \min_{O^\top O = I_3} \sum_{i=1}^N \|\hat{R}_i - O\tilde{R}_i\|_F^2.$$

We compare IDDM with RSlocal and the eigenvector relaxation method developed in [31] (dubbed as “eigs”). The semidefinite programming relaxation approach in [31] is not compared because our experiments show that our local algorithm often can be better than it in terms of both accuracy and computational time. Each run of IDDM consists of ten cycles starting from the point generated from eigs while RSlocal is made up of ten trials of the local algorithm starting either from eigs or nine randomly generated points. The parameter  $\alpha$  in IDDM is set to 0.1. In the subsequent experiments, “cpu” is the average cpu time of one cycle in seconds and “obj” stands for the final objective value.

Our first experiment is based on randomly generated data sets. We first create  $N$  rotations  $\tilde{R}_i$  by using the MATLAB command “orth(rand(3,3))”. The common line vectors are computed next as  $\tilde{c}_{ij} = \tilde{R}_i^{-1} \cdot (\tilde{R}_i^3 \times \tilde{R}_j^3) / \|\tilde{R}_i^3 \times \tilde{R}_j^3\|$  and  $\tilde{c}_{ji} = \tilde{R}_j^{-1} \cdot (\tilde{R}_j^3 \times \tilde{R}_i^3) / \|\tilde{R}_j^3 \times \tilde{R}_i^3\|$  from each pair  $\tilde{R}_i$  and  $\tilde{R}_j$ . After converting  $\tilde{c}_{ij}$  and  $\tilde{c}_{ji}$  into  $c_{ij}$  and  $c_{ji}$ , we replace  $c_{ij}$  and  $c_{ji}$  by two random vectors that are sampled from the uniform distribution over the unit circle with probability  $p$ . That is, the common line vectors stay the same with probability  $(1 - p)$ . We test the cases of  $N = 100, 500, 1000$ . The computed objective function values are presented in the left column of Figure 3. The lines “eigs”, “IDDM mean” and “IDDM min” are the objective function value computed by eigs, the averaged and minimum objective function value computed by IDDM, respectively. The lines “RSlocal mean” and “RSlocal min” are the corresponding values of RSlocal. We can see that both RSlocal and IDDM can find better objective function values than eigs. We should point that both RSlocal and IDDM can find the same minimum when they start from the initial point generated by eigs. However, IDDM performs better than RSlocal on average.

A detailed summary of the computational results are reported in Table 5. We further denote “mse1” as the smallest MSE generated in the ten cycles and “obj1” is the corresponding objective function value. Similarly, “obj2” stands the smallest objective value in ten cycles and the corresponding MSE is denoted as “mse2”. We can see that the pairs “(mse1, obj1)” and “(mse2, obj2)” are almost the same except the last row of each of  $N = 100, 500, 1000$ . The reason is that the initial point produced

by eigs lies in a small neighbourhood of the global solution and our local algorithm starting from eigs usually can find this global solution successfully. Although other cycles can also identify a local solution, the corresponding objective function values are larger. For the cases that mse1 is different from mse2, it means that a smaller objective function value does not necessary have a smaller MSE in the noisy cases. The reason is that the model (60) does not characterize the original Cryo-EM problem well.

Our second experiment is based on the dataset from [31]. The noise-to-signal ratio (NSR) is defined as  $NSR = \text{Var}(Noise)/\text{Var}(Signal)$ , where *Signal* is the clean projection image and *Noise* is the noise realization. The set up of the experiments is the same as the random data sets. The objective function values are plotted in the right column of Figure 3. They show that eigs itself can provide a good solution when NSR is small. The averaged objective function values obtained from IDDM are the best when NSR is larger. IDDM also can find a smaller objective function value in a few cases. The detailed summary of computational results are presented in Table 6. The pairs “(mse1, obj1)” and “(mse2, obj2)” are almost the same when NSR is small. However, for a large NSR, IDDM often is able to identify a smaller objective function value whose corresponding MSE is not the best. This observation again is not a contradiction but due to that the model (60) is not suitable in these cases. Nevertheless, these experiments are still perfect to show that IDDM is often better than the local algorithm itself and the local algorithm starting from multiple randomly generated initial points when the global solution is difficult to be captured.

**6. Conclusion.** The goal of this paper is to construct an algorithm which is able to identify global solutions of minimization with orthogonality constraints. Our strategy is simply alternating between a local algorithm on Stiefel manifold and a gradient flow method with stochastic diffusion on manifold. The main concept is that a suitable diffusion term is able to drive the iteration to escape the region around a local solution. We derive an extrinsic form of the Brownian motion on the manifold and design a numerical efficient scheme to solve the corresponding SDE on manifold. We further theoretically show the half order convergence of the proposed numerical method for solving SDE on the Stiefel manifold. Moreover, convergence to the global minimizer is also theoretically established as long as the diffusion is sufficiently enough. However, our extensive numerical experiments on polynomial optimization and 3D structure determination from Cryo-EM show that a few cycles of our algorithm is often able to provide a better solution than the local algorithm. Although both theoretical and numerical results are still limited in certain senses, they are indeed promising especially for problems with good structures. Our future work includes a better theoretical understanding the algorithms, refining them for more typical applications and some better ways on choosing or even learning the diffusion parameter  $\sigma(t)$ .

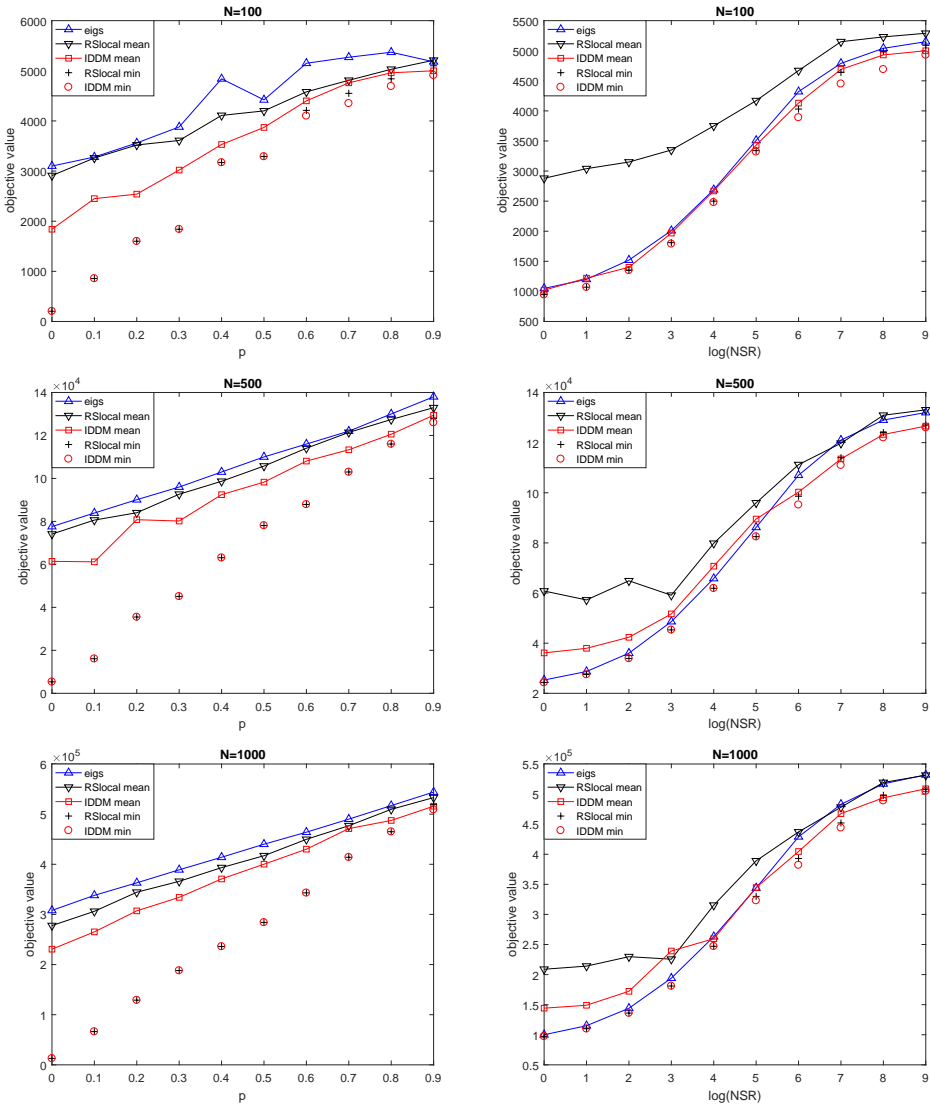


FIG. 3. The objective values for the random datasets (left column) and the dataset from [31] (right column)

TABLE 3  
*Numerical results of biquadratic optimization: case ii*

$n$	RSlocal				IDDM			
	min	mean	max	cpu	min	mean	max	cpu
6	4.0e-14	3.6e-04	5.9e-03	0.014	4.7e-14	3.6e-04	5.9e-03	0.020
7	3.2e-14	7.1e-03	1.2e-01	0.016	4.2e-14	1.1e-13	2.8e-13	0.016
8	0.0e+00	8.3e-03	8.8e-02	0.032	4.9e-15	2.4e-03	4.0e-02	0.042
9	5.6e-14	7.0e-02	4.2e-01	0.020	2.3e-14	2.2e-02	4.2e-01	0.028
10	2.0e-14	6.7e-02	2.4e-01	0.029	1.4e-14	3.5e-02	1.8e-01	0.040
11	9.5e-14	7.4e-03	7.1e-02	0.031	6.8e-14	2.4e-03	6.3e-03	0.046
12	1.2e-13	4.6e-02	2.3e-01	0.036	4.4e-14	2.0e-12	2.0e-11	0.045
13	1.4e-13	5.2e-02	2.7e-01	0.039	4.3e-14	2.5e-02	2.9e-01	0.061
14	5.7e-14	2.9e-01	8.2e-01	0.056	3.5e-14	1.0e-01	7.1e-01	0.084
15	7.1e-15	6.0e-02	2.7e-01	0.064	3.8e-14	2.7e-02	3.0e-01	0.092
16	3.6e-14	1.3e-01	9.2e-01	0.091	5.0e-14	2.0e-12	3.1e-12	0.125
17	3.5e-14	5.6e-02	7.8e-01	0.091	1.3e-14	5.1e-13	7.6e-12	0.141
18	2.3e-13	2.8e-01	8.0e-01	0.118	5.4e-14	8.9e-14	1.5e-13	0.165
19	1.4e-13	1.1e-01	4.5e-01	0.146	1.2e-14	9.3e-02	2.7e-01	0.232
20	6.8e-14	1.8e-01	7.0e-01	0.202	2.4e-13	1.2e-01	7.1e-01	0.282
21	1.5e-13	1.3e-01	3.7e-01	0.235	3.6e-14	9.4e-02	2.3e-01	0.366
22	1.8e-13	2.3e-01	5.5e-01	0.291	7.0e-13	1.4e-01	5.1e-01	0.469
23	1.0e-12	1.3e-01	4.8e-01	0.360	5.6e-13	1.1e-01	5.1e-01	0.550
24	1.1e-12	2.1e-01	4.8e-01	0.389	9.9e-14	1.9e-02	4.2e-01	0.610
25	9.4e-13	9.6e-02	3.4e-01	0.507	0.0e+00	8.7e-02	3.3e-01	0.771



TABLE 4  
Stability Number

graph		RSlocal			IDDM		
name	$ V $	mean	max	cpu (s)	mean	max	cpu (s)
theta10	500	47.0	50	0.686	47.0	51	0.620
theta12	600	49	50	0.949	49	54	0.872
theta42	200	15	17	0.254	15.5	18	0.265
G43	1000	180.5	188	0.671	189.0	195	0.497
G44	1000	182.0	190	0.654	191.0	199	0.503
G45	1000	179.0	188	0.667	187.5	197	0.495
G46	1000	180.0	186	0.651	189.0	196	0.505
G47	1000	184.0	190	0.689	191.5	200	0.487
G51	1000	332.0	336	0.813	343.0	346	0.603
G52	1000	330.0	335	0.837	341.0	344	0.616
G53	1000	330.0	334	0.783	340.0	343	0.557
G54	1000	323.0	330	0.725	334.0	339	0.532
sanr200-0.7	200	16.0	17	0.262	15.0	18	0.275
brock200-4	200	14.0	15	0.273	14.0	17	0.275
hamming-6-4	64	4.0	4	0.033	4.0	4	0.032
hamming-9-8	512	168.0	179	0.264	173.0	186	0.089
hamming-10-2	1024	65.0	67	0.911	66.0	70	0.844
hamming-11-2	2048	113.0	116	2.267	118.0	122	1.889
keller4	171	9.0	11	0.247	11.0	11	0.172
fap25	2118	78.0	80	29.471	79.0	82	25.063
1dc.1024	1024	69.0	71	1.092	70.0	73	1.006
1dc.2048	2048	119.0	123	2.679	125.0	129	2.290
1et.512	512	91.0	96	0.202	92.0	96	0.175
1et.1024	1024	154.0	158	0.426	159.0	162	0.363
1et.2048	2048	270.0	275	0.971	289.0	296	0.894
1tc.512	512	101.0	104	0.165	103.0	106	0.156
1tc.1024	1024	174.0	180	0.357	183.0	187	0.302
1tc.2048	2048	305.0	312	0.804	323.5	329	0.740
1zc.512	512	51.0	54	0.299	51.5	55	0.286
1zc.1024	1024	91.0	95	0.728	93.0	99	0.648
1zc.2048	2048	160.0	164	1.740	169.0	175	1.388
1zc.4096	4096	286.0	292	4.502	289.0	296	4.673
2dc.512	512	10.0	10	2.303	10.0	11	2.001

TABLE 5  
*The MSE of the eigenvector, RSlocal and IDDM for random dataset*

P	eigs		local				IDDM					
	mse	obj	mse1, obj1		mse2, obj2		cpu	mse1, obj1		mse2, obj2		cpu
N=100												
1.0	3.45e-1	3.10e3	1.19e-4	2.04e2	1.19e-4	2.04e2	0.7	1.19e-4	2.04e2	1.19e-4	2.04e2	0.8
0.9	3.31e-1	3.28e3	9.98e-4	8.57e2	9.98e-4	8.57e2	0.7	9.98e-4	8.57e2	9.98e-4	8.57e2	0.8
0.8	3.77e-1	3.56e3	7.01e-3	1.60e3	7.01e-3	1.60e3	0.7	7.01e-3	1.60e3	7.01e-3	1.60e3	0.7
0.7	3.97e-1	3.88e3	3.86e-3	1.84e3	3.86e-3	1.84e3	0.7	3.86e-3	1.84e3	3.86e-3	1.84e3	0.7
0.6	2.18	4.84e3	1.25	3.17e3	1.25	3.17e3	0.5	9.78e-1	3.26e3	1.25	3.17e3	0.6
0.5	7.00e-1	4.42e3	1.91e-1	3.29e3	1.91e-1	3.29e3	0.4	1.91e-1	3.29e3	1.91e-1	3.29e3	0.5
0.4	2.89	5.15e3	1.98	4.21e3	1.98	4.21e3	0.5	1.67	4.10e3	1.67	4.10e3	0.6
0.3	3.45	5.27e3	2.23	4.75e3	2.70	4.55e3	0.5	2.12	4.35e3	2.12	4.35e3	0.5
0.2	3.56	5.37e3	2.53	4.84e3	2.53	4.84e3	0.5	2.28	4.69e3	2.28	4.69e3	0.5
0.1	4.27	5.18e3	2.67	5.22e3	4.25	5.10e3	0.5	3.60	4.91e3	3.60	4.91e3	0.5
N=500												
1.0	3.42e-1	7.76e4	1.33e-4	5.35e3	1.33e-4	5.35e3	9.8	1.33e-4	5.35e3	1.33e-4	5.35e3	9.9
0.9	3.42e-1	8.39e4	4.98e-6	1.61e4	4.98e-6	1.61e4	9.9	4.98e-6	1.61e4	4.98e-6	1.61e4	8.5
0.8	3.40e-1	9.01e4	9.34e-4	3.55e4	9.34e-4	3.55e4	6.4	9.34e-4	3.55e4	9.34e-4	3.55e4	7.1
0.7	3.35e-1	9.60e4	3.42e-5	4.51e4	3.42e-5	4.51e4	6.3	3.42e-5	4.51e4	3.42e-5	4.51e4	7.4
0.6	3.74e-1	1.03e5	2.56e-3	6.31e4	2.56e-3	6.31e4	5.9	2.56e-3	6.31e4	2.56e-3	6.31e4	6.8
0.5	3.74e-1	1.10e5	6.28e-3	7.81e4	6.28e-3	7.81e4	5.6	6.28e-3	7.81e4	6.28e-3	7.81e4	5.9
0.4	3.89e-1	1.16e5	7.45e-3	8.79e4	7.45e-3	8.79e4	5.0	7.45e-3	8.79e4	7.45e-3	8.79e4	5.5
0.3	4.54e-1	1.22e5	2.22e-2	1.03e5	2.22e-2	1.03e5	4.3	2.22e-2	1.03e5	2.22e-2	1.03e5	5.2
0.2	8.04e-1	1.30e5	1.35e-1	1.16e5	1.35e-1	1.16e5	4.0	1.35e-1	1.16e5	1.35e-1	1.16e5	4.8
0.1	4.03	1.38e5	2.67	1.33e5	3.42	1.28e5	4.3	2.59	1.26e5	2.59	1.26e5	4.8
N=1000												
1.0	3.34e-1	3.08e5	1.43e-5	1.28e4	1.43e-5	1.28e4	163	1.43e-5	1.28e4	1.43e-5	1.28e4	87
0.9	3.51e-1	3.38e5	8.13e-6	6.63e4	8.13e-6	6.63e4	113	8.13e-6	6.63e4	8.13e-6	6.63e4	49
0.8	3.51e-1	3.63e5	9.46e-5	1.29e5	9.46e-5	1.29e5	103	9.46e-5	1.29e5	9.46e-5	1.29e5	57
0.7	3.54e-1	3.89e5	3.20e-4	1.88e5	3.20e-4	1.88e5	91	3.20e-4	1.88e5	3.20e-4	1.88e5	42
0.6	3.59e-1	4.14e5	1.51e-4	2.36e5	1.51e-4	2.36e5	84	1.51e-4	2.36e5	1.51e-4	2.36e5	33
0.5	3.67e-1	4.40e5	2.47e-5	2.84e5	2.47e-5	2.84e5	57	2.47e-5	2.84e5	2.47e-5	2.84e5	35
0.4	3.61e-1	4.64e5	1.05e-3	3.43e5	1.05e-3	3.43e5	50	1.05e-3	3.43e5	1.05e-3	3.43e5	27
0.3	3.97e-1	4.90e5	1.31e-2	4.14e5	1.31e-2	4.14e5	34	1.31e-2	4.14e5	1.31e-2	4.14e5	23
0.2	5.26e-1	5.17e5	5.00e-2	4.65e5	5.00e-2	4.65e5	18	5.00e-2	4.65e5	5.00e-2	4.65e5	18
0.1	2.24	5.44e5	1.44	5.25e5	2.61	5.19e5	19	1.44	5.25e5	3.91	5.09e5	18

TABLE 6  
*The MSE of the eigenvector, RSlocal and IDDM for dataset from [31]*

NSR	eigs		RSlocal				IDDM					
	mse	obj	mse1, obj1		mse2, obj2		cpu	mse1, obj1		mse2, obj2		cpu
N=100												
1	3.00e-3	1.05e3	3.04e-4	9.47e2	3.04e-4	9.47e2	0.5	2.99e-4	9.47e2	3.04e-4	9.47e2	0.5
2	4.41e-3	1.20e3	5.04e-4	1.07e3	5.04e-4	1.07e3	0.5	4.95e-4	1.07e3	5.15e-4	1.07e3	0.5
4	1.06e-2	1.52e3	1.60e-3	1.35e3	1.60e-3	1.35e3	0.5	1.07e-3	1.35e3	1.10e-3	1.35e3	0.5
8	2.88e-2	2.01e3	6.19e-3	1.81e3	6.19e-3	1.81e3	0.6	3.38e-3	1.79e3	3.38e-3	1.79e3	0.5
16	8.81e-2	2.69e3	3.77e-2	2.50e3	3.77e-2	2.50e3	0.6	3.04e-2	2.48e3	3.12e-2	2.48e3	0.5
32	2.63e-1	3.51e3	1.88e-1	3.34e3	1.88e-1	3.34e3	0.5	1.88e-1	3.34e3	2.07	3.32e3	0.4
64	2.60	4.32e3	2.30	4.03e3	2.30	4.03e3	0.5	2.30	4.03e3	2.40	3.89e3	0.4
128	3.28	4.79e3	3.08	4.64e3	3.08	4.64e3	0.4	3.08	4.64e3	3.40	4.45e3	0.4
256	4.10	5.04e3	4.05	4.99e3	4.05	4.99e3	0.4	4.05	4.99e3	4.19	4.69e3	0.4
512	4.97	5.15e3	4.98	5.09e3	4.98	5.09e3	0.4	4.86	5.03e3	5.16	4.93e3	0.4
N=500												
1	1.20e-3	2.53e4	1.54e-4	2.43e4	1.54e-4	2.43e4	16	1.54e-4	2.43e4	1.54e-4	2.43e4	7.8
2	1.77e-3	2.87e4	2.94e-4	2.75e4	2.94e-4	2.75e4	17	2.94e-4	2.75e4	2.94e-4	2.75e4	11
4	5.10e-3	3.60e4	7.58e-4	3.39e4	7.58e-4	3.39e4	16	7.07e-4	3.39e4	7.07e-4	3.39e4	7.1
8	1.91e-2	4.86e4	3.14e-3	4.53e4	3.14e-3	4.53e4	17	3.14e-3	4.53e4	3.14e-3	4.53e4	7.1
16	6.35e-2	6.58e4	1.81e-2	6.19e4	1.81e-2	6.19e4	8.7	1.81e-2	6.19e4	1.81e-2	6.19e4	7.6
32	2.18e-1	8.62e4	1.34e-1	8.25e4	1.34e-1	8.25e4	5.5	1.34e-1	8.25e4	1.34e-1	8.25e4	6.8
64	1.75	1.07e5	1.61	9.86e4	1.61	9.86e4	5.6	1.61	9.86e4	2.23	9.52e4	9.3
128	2.62	1.21e5	2.32	1.14e5	2.32	1.14e5	5.7	2.32	1.14e5	2.84	1.11e5	8.8
256	3.49	1.29e5	3.22	1.24e5	3.22	1.24e5	5.0	3.22	1.24e5	4.18	1.22e5	5.5
512	4.59	1.32e5	4.65	1.32e5	4.84	1.27e5	6.1	4.58	1.26e5	4.58	1.26e5	5.9
N=1000												
1	8.27e-4	1.00e5	1.25e-4	9.73e4	1.25e-4	9.73e4	59	1.25e-4	9.73e4	1.25e-4	9.73e4	51
2	1.46e-3	1.15e5	2.58e-4	1.10e5	2.58e-4	1.10e5	75	2.58e-4	1.10e5	2.58e-4	1.10e5	67
4	4.56e-3	1.44e5	6.60e-4	1.36e5	6.60e-4	1.36e5	65	6.60e-4	1.36e5	6.60e-4	1.36e5	58
8	1.81e-2	1.94e5	2.46e-3	1.81e5	2.46e-3	1.81e5	60	2.46e-3	1.81e5	2.46e-3	1.81e5	45
16	6.41e-2	2.63e5	1.43e-2	2.47e5	1.43e-2	2.47e5	43	1.43e-2	2.47e5	1.43e-2	2.47e5	55
32	2.32e-1	3.44e5	1.43e-1	3.30e5	1.43e-1	3.30e5	28	1.43e-1	3.30e5	2.09	3.23e5	35
64	1.78	4.29e5	1.64	3.93e5	1.64	3.93e5	32	1.64	3.93e5	2.24	3.82e5	37
128	2.50	4.83e5	2.24	4.52e5	2.24	4.52e5	36	2.24	4.52e5	2.67	4.44e5	30
256	3.48	5.17e5	3.21	4.98e5	3.21	4.98e5	33	3.21	4.98e5	4.10	4.89e5	37
512	4.62	5.32e5	4.62	5.32e5	4.79	5.08e5	30	4.62	5.32e5	4.86	5.05e5	29

## REFERENCES

- [1] P. A. ABSIL, R. MAHONY, AND R. SEPULCHRE, *Optimization algorithms on matrix manifolds*, Princeton University Press, Princeton, NJ, 2008, doi:10.1515/9781400830244.
- [2] M. AHARON, M. ELAD, AND A. BRUCKSTEIN, *rmk-svd: An algorithm for designing overcomplete dictionaries for sparse representation*, IEEE Transactions on signal processing, 54 (2006), pp. 4311–4322.
- [3] F. ALUFFI-PENTINI, V. PARISI, AND F. ZIRILLI, *Global optimization and stochastic differential equations*, Journal of optimization theory and applications, 47 (1985), pp. 1–16, doi:10.1007/BF00941312.
- [4] P. T. BOUFOUNOS AND R. G. BARANIUK, *1-bit compressive sensing*, in Information Sciences and Systems, 2008. CISS 2008. 42nd Annual Conference on, IEEE, 2008, pp. 16–21.
- [5] J.-F. CAI, H. JI, Z. SHEN, AND G.-B. YE, *Data-driven tight frame construction and image denoising*, Applied and Computational Harmonic Analysis, 37 (2014), pp. 89–105.
- [6] T.-S. CHIANG, C.-R. HWANG, AND S. J. SHEU, *Diffusion for Global Optimization in  $\mathbb{R}^n$* , SIAM Journal on Control and Optimization, 25 (1987), pp. 737–753, doi:10.1137/0325042.
- [7] S.-N. CHOW, T.-S. YANG, AND H.-M. ZHOU, *GLOBAL OPTIMIZATIONS BY INTERMITTENT DIFFUSION*, in Chaos, CNN, Memristors and Beyond, WORLD SCIENTIFIC, Feb. 2013, pp. 466–479, doi:10.1142/9789814434805\_0037.
- [8] A. EDELMAN, T. A. ARIAS, AND S. T. SMITH, *The Geometry of Algorithms with Orthogonality Constraint*, SIAM Journal on Matrix Analysis and Applications, 20 (1998), pp. 303–353, doi:10.1137/S0895479895290954.
- [9] S. GEMAN AND C.-R. HWANG, *Diffusions for Global Optimization*, SIAM Journal on Control and Optimization, 24 (1986), pp. 1031–1043, doi:10.1137/0324060.
- [10] B. GIDAS, *Global optimization via the Langevin equation*, in 1985 24th IEEE Conference on Decision and Control, IEEE, 1985, pp. 774–778, doi:10.1109/CDC.1985.268602.
- [11] D. GOLDFARB, Z. WEN, AND W. YIN, *A curvilinear search method for p-harmonic flows on spheres*, SIAM Journal on Imaging Sciences, 2 (2009), pp. 84–109.
- [12] X. GU AND S.-T. YAU, *Global conformal surface parameterization*, in Proceedings of the 2003 Eurographics/ACM SIGGRAPH symposium on Geometry processing, Eurographics Association, 2003, pp. 127–137.
- [13] O. HENKEL, *Sphere-Packing Bounds in the Grassmann and Stiefel Manifolds*, Institute of Electrical and Electronics Engineers. Transactions on Information Theory, 51 (2005), pp. 3445–3456, doi:10.1109/TIT.2005.855594.
- [14] E. HSU, *Stochastic Analysis on Manifolds*, vol. 38 of Graduate Studies in Mathematics, American Mathematical Society, Providence, Rhode Island, Feb. 2002, doi:10.1090/gsm/038.
- [15] R. LAI, Z. WEN, W. YIN, X. GU, AND L. M. LUI, *Folding-free global conformal mapping for genus-0 surfaces by harmonic energy minimization*, Journal of Scientific Computing, 58 (2014), pp. 705–725.
- [16] J. N. LASKA, Z. WEN, W. YIN, AND R. G. BARANIUK, *Trust, but verify: Fast and accurate signal recovery from 1-bit compressive measurements*, IEEE Transactions on Signal Processing, 59 (2011), pp. 5289–5301.
- [17] S.-Y. LIN AND M. LUSKIN, *Relaxation methods for liquid crystal problems*, SIAM Journal on Numerical Analysis, 26 (1989), pp. 1310–1324.
- [18] C. LING, J. NIE, L. QI, AND Y. YE, *Biquadratic optimization over unit spheres and semidefinite programming relaxations*, SIAM J. Optim., 20 (2009), pp. 1286–1310, doi:10.1137/080729104.
- [19] X. LIU, Z. WEN, X. WANG, M. ULBRICH, AND Y. YUAN, *On the analysis of the discretized Kohn-Sham density functional theory*, SIAM J. Numer. Anal., 53 (2015), pp. 1758–1785, doi:10.1137/140957962.
- [20] D. MARINGER AND P. PAPPAS, *Global optimization of higher order moments in portfolio selection*, Journal of Global Optimization, 43 (2007), pp. 219–230, doi:10.1007/s10898-007-9224-3.
- [21] P. A. MARKOWICH AND C. VILLANI, *On the trend to equilibrium for the Fokker-Planck equation: an interplay between physics and functional analysis*, Matemática Contemporânea, 19 (2000), pp. 1–29.
- [22] T. S. MOTZKIN AND E. G. STRAUS, *Maxima for graphs and a new proof of a theorem of Turán*, Canadian Journal of Mathematics. Journal Canadien de Mathématiques, 17 (1965), pp. 533–540, doi:10.4153/CJM-1965-053-6.
- [23] J. NOCEDAL AND S. J. WRIGHT, *Numerical Optimization*, Springer Series in Operations Research and Financial Engineering, Springer, New York, second ed., 2006.
- [24] B. Ø KSENDAL, *Stochastic differential equations*, Universitext, Springer-Verlag, Berlin, Berlin,

- Heidelberg, sixth ed., 2003, doi:10.1007/978-3-642-14394-6.
- [25] J. OPREA, *Differential geometry and its applications*, Classroom Resource Materials Series, Mathematical Association of America, Washington, DC, second ed., 2007.
  - [26] V. OZOLIŅŠ, R. LAI, R. CAFLISCH, AND S. OSHER, *Compressed modes for variational problems in mathematics and physics*, Proceedings of the National Academy of Sciences, 110 (2013), pp. 18368–18373.
  - [27] P. PAPPAS AND B. RUSTEM, *An Algorithm for the Global Optimization of a Class of Continuous Minimax Problems*, Journal of optimization theory and applications, 141 (2008), pp. 461–473, doi:10.1007/s10957-008-9473-4.
  - [28] P. PAPPAS AND B. RUSTEM, *Convergence analysis of a global optimization algorithm using stochastic differential equations*, Journal of Global Optimization, 45 (2009), pp. 95–110, doi:10.1007/s10898-008-9397-4.
  - [29] P. PAPPAS, B. RUSTEM, AND E. N. PISTIKOPOULOS, *Linearly Constrained Global Optimization and Stochastic Differential Equations*, Journal of Global Optimization, 36 (2006), pp. 191–217, doi:10.1007/s10898-006-9026-z.
  - [30] P. PAPPAS, B. RUSTEM, AND E. N. PISTIKOPOULOS, *Global optimization of robust chance constrained problems*, Journal of Global Optimization, 43 (2007), pp. 231–247, doi:10.1007/s10898-007-9244-z.
  - [31] A. SINGER AND Y. SHKOLNISKY, *Three-Dimensional Structure Determination from Common Lines in Cryo-EM by Eigenvectors and Semidefinite Programming*, SIAM Journal on Imaging Sciences, 4 (2011), pp. 543–572, doi:10.1137/090767777.
  - [32] B. TANG, G. SAPIRO, AND V. CASELLES, *Color image enhancement via chromaticity diffusion*, IEEE Transactions on Image Processing, 10 (2001), pp. 701–707.
  - [33] L. A. VESE AND S. J. OSHER, *Numerical methods for  $p$ -harmonic flows and applications to image processing*, SIAM Journal on Numerical Analysis, 40 (2002), pp. 2085–2104.
  - [34] C. VILLANI, *Optimal Transport*, vol. 338 of Grundlehren der mathematischen Wissenschaften, Springer Berlin Heidelberg, Berlin, Heidelberg, 2009, doi:10.1007/978-3-540-71050-9.
  - [35] Z. WEN, A. MILZAREK, M. ULBRICH, AND H. ZHANG, *Adaptive regularized self-consistent field iteration with exact Hessian for electronic structure calculation*, SIAM J. Sci. Comput., 35 (2013), pp. A1299–A1324, doi:10.1137/120894385.
  - [36] Z. WEN AND W. YIN, *A feasible method for optimization with orthogonality constraints*, Mathematical programming, 142 (2012), pp. 397–434, doi:10.1007/s10107-012-0584-1.
  - [37] G. YIN AND K. YIN, *Global Optimization Using Diffusion Perturbations with Large Noise Intensity*, Acta Mathematicae Applicatae Sinica, English Series, 22 (2006), pp. 529–542, doi:10.1007/s10255-006-0328-1.